

This is a repository copy of Regulation of LRRK2 activity by metabolic stress and heavy metal exposure.

White Rose Research Online URL for this paper: https://eprints.whiterose.ac.uk/id/eprint/233152/

Version: Published Version

Article:

Kentros, M., Follett, J., Subrahmanian, N. orcid.org/0000-0003-2975-4271 et al. (12 more authors) (2025) Regulation of LRRK2 activity by metabolic stress and heavy metal exposure. Brain Research, 1863. 149785. ISSN: 0006-8993

https://doi.org/10.1016/j.brainres.2025.149785

Reuse

This article is distributed under the terms of the Creative Commons Attribution (CC BY) licence. This licence allows you to distribute, remix, tweak, and build upon the work, even commercially, as long as you credit the authors for the original work. More information and the full terms of the licence here: https://creativecommons.org/licenses/

Takedown

If you consider content in White Rose Research Online to be in breach of UK law, please notify us by emailing eprints@whiterose.ac.uk including the URL of the record and the reason for the withdrawal request.



ELSEVIER

Contents lists available at ScienceDirect

Brain Research

journal homepage: www.elsevier.com/locate/brainres



Research paper

Regulation of LRRK2 activity by metabolic stress and heavy metal exposure



Michalis Kentros^a, Jordan Follett^{b,c}, Nitya Subrahmanian^{b,c}, Aravindraja Chairmandurai ^{b,c}, Katerina Melachroinou^a, Diane B. Re^d, Rafael de Cabo^e, Ruth Chia^f, Jillian H. Kluss^g, Alexandra Beilina^g, Heather Mortiboys^h, Matthew J. LaVoie^{b,c}, Hardy J. Rideout^a, Mark R. Cookson^g, Adamantios Mamais^{b,c,*}

- a Center for Clinical, Experimental Surgery, & Translational Research, Biomedical Research Foundation of the Academy of Athens, Greece
- ^b Department of Neurology, McKnight Brain Institute, University of Florida, Gainesville, FL, USA
- ^c Center for Translational Research in Neurodegenerative Disease and Fixel Institute for Neurologic Diseases, Department of Neurology, University of Florida, Gainesville, FL, USA
- d Department of Environmental Health Sciences, Mailman School of Public Health, Columbia University, New York, NY, USA
- e Translational Gerontology Branch, NIA, NIH, MD, USA
- f Neuromuscular Diseases Research Section, National Institute on Aging, Bethesda, MD, USA
- g Cell Biology and Gene Expression Section, NIA, NIH, MD, USA
- h Sheffield Institute for Translational Neuroscience (SITraN), University of Sheffield, Sheffield, United Kingdom

ARTICLE INFO

Keywords: LRRK2 Manganese Metabolic stress

ABSTRACT

Genetic variability in the gene encoding leucine-rich repeat kinase 2 (LRRK2) is associated with both familial and sporadic Parkinson's disease (PD). While LRRK2 is known to modulate vesicular trafficking and stress signaling through its phosphorylation and kinase activity, how it responds to metabolic and environmental stressors remains poorly understood. Here, we show that acute inhibition of glycolysis and oxidative phosphorylation triggers rapid, reversible dephosphorylation of LRRK2 at constitutive sites in cells, ex vivo brain slices, and primary astrocytes. In contrast, glucose deprivation modestly increases LRRK2 kinase activity and Rab substrate phosphorylation. In vivo, chronic 2-deoxyglucose treatment reduces S935 phosphorylation in kidney tissue, linking energy stress to LRRK2 modulation in peripheral organs. Strikingly, manganese (Mn), a PD-relevant environmental toxicant, robustly activates LRRK2, inducing pS1292 autophosphorylation and phosphorylation of Rab8a, Rab10 and Rab12, while suppressing S935 phosphorylation after a 24 hrs exposure. Time-resolved analysis revealed distinct temporal substrate regulation, with rapid Rab12 phosphorylation and pRab10 levels gradually increasing and peaking only after 24 h. Phosphorylated Rab10 remains closely associated with both lysosomal and centrosomal membranes under Mn stress. Mn impaired mitochondrial respiration and increased ROS, and antioxidant treatment rescued Rab10 phosphorylation, establishing a redox-dependent mechanism of LRRK2 activation. Together, these findings reveal stressor-specific modes of LRRK2 regulation and suggest that LRRK2 integrates metabolic and environmental signals via redox-sensitive pathways relevant to PD pathogenesis.

1. Introduction

Leucine-rich Repeat Kinase 2 (LRRK2) has been associated with both inherited and idiopathic Parkinson's disease (PD) with genetic variability documented in and around the gene (Kluss et al., 2019). LRRK2 is a phospho-protein and its phosphorylation is believed to be important in its role in disease pathology. PD-linked mutations on LRRK2 affect its phosphorylation at Ser910 and Ser935 suggesting that signaling events that control its constitutive phosphorylation are linked to PD (Nichols

et al., 2010). The kinase activity of LRRK2 towards a subset of Rab GTPases substrates is augmented by PD-linked mutations (Steger, et al., 2016; Beilina, 2014; Mamais et al., 2024; Pfeffer, 2023), highlighting the need to understand the cellular pathways that modulate its phosphorylation and activity. Despite the identification of Casein kinase α (CK1 α) and TANK-binding kinase 1 (TBK1) signaling regulating its phosphorylation (Chia, 2014; Dzamko, 2012), as well as protein phosphatase 1 and 2A (PP1, PP2A) as LRRK2 phosphatases (Lobbestael et al., 2013), there is much to characterize around how age-related pathways

E-mail address: a.mamais@ufl.edu (A. Mamais).

^{*} Corresponding author.

and cellular stress modulate LRRK2. Importantly, oxidative stress has been nominated as a driver of LRRK2 activity in vivo linking metabolic dyshomeostasis in aging to LRRK2 signaling (Di Maio, 2018; Yang, 2012). We, and others, have previously proposed cellular oxidative stress as a modulator of LRRK2 phosphorylation and activity (Di Maio, 2018; Mamais et al., 2014). Studies have reported mitochondrial abnormalities in the striatum of homozygous G2019S knock-in mice (Yue, 2015), the most common LRRK2 mutation in PD. In a similar fashion, compromised mitochondrial function was reported in fibroblasts and iPSC-derived neurons from G2019S LRRK2 carriers (Mortiboys et al., 2015; Hsieh, 2016). Studies reported dysregulated mitochondrial membrane potential induced by expression of G2019S LRRK2 in cells (Papkovskaia et al., 2012) while recent data link LRRK2 activity to ROS production in cells (Keeney, 2024). These studies support a model whereby LRRK2 function in neuropathology is linked to mitochondrial dysfunction placing control of LRRK2 activity in signaling pathways of metabolism and energy homeostasis. While our previous work highlighted arsenite as a modulator of LRRK2 phosphorylation and activity in cells, arsenite treatment impairs diverse cellular pathways raising important questions on the specific signaling that affects LRRK2. Arsenite impairs ATP production by inhibiting pyruvate dehydrogenase and drives H₂O₂ accumulation leading to nitric oxide and reactive oxygen species (ROS) increase in cells. To extend this work, we set out to explore how LRRK2 is modulated by metabolic stress focusing on mitochondrial and glycolytic energy production. By using specific inhibitors as well as exposure to manganese, a trace metal that disrupts cellular energy metabolism and has been linked to parkinsonism (Diessl, 2022; Harischandra, 2019; Kwakye et al., 2015). Inhibiting glycolysis and oxidative phosphorylation in culture and ex vivo mouse striatal slices induced a reduction in LRRK2 constitutive phosphorylation. Mitochondrial depolarization was not sufficient or required for LRRK2 dephosphorylation but depletion of intracellular ATP levels induced changes in LRRK2 phosphorylation, in an AMPK-independent manner. In rats, chronic administration of 2-Deoxy-D-Glucose (2DG) induced pS935 loss in kidney tissue. Interestingly, glucose deprivation in culture induced a mild activation of LRRK2 activity while 2DG treatment did not recapitulate the effect. We examined the localization of Rab8a, a LRRK2 substrate, in mutant LRRK2 mouse astrocytes in conditions of metabolic stress. Rab8a associates with tubular recycling endosomes and mediates receptor recycling (Kobayashi et al., 2014; Sharma et al., 2009; Mamais et al., 2021). LRRK2 mutant astrocytes exhibited shorter Rab8a-positive tubular endosomes, suggesting a role of LRRK2 in vesicular trafficking in metabolic stress conditions. Lastly, we explored manganese exposure as a PD-relevant metal that affects endosomal dynamics, mitochondrial function and cellular energy metabolism (Diessl, 2022; Kwakye et al., 2015; Smith et al., 2017). Consistent with previously published reports, manganese treatment induced LRRK2 activation with an increase in autophosphorylation and Rab GTPase phosphorylation in cells. Interestingly, our data support temporal regulation and substrate-specific signaling dynamics with rapid phosphorylation of Rab12 and delayed Rab10 phosphorylation under manganese treatment. Manganese impaired mitochondrial function and induced ROS, while antioxidant treatment rescued LRRK2 activation and Rab10 phosphorylation. Our data place LRRK2 activation and phosphorylation in pathways that are responsive to metabolic dyshomeostasis and heavy metal exposure and highlight signaling targets of therapeutic intervention.

2. Results

2.1. Metabolic stress induces loss of LRRK2 constitutive phosphorylation

We, and others, have shown that LRRK2 phosphorylation can be affected by ROS and arsenite stress in cells (Di Maio, 2018; Mamais et al., 2014), highlighting metabolic and energy homeostasis pathways as modulators of LRRK2 signaling. To investigate the effect of impaired energy homeostasis on LRRK2, we targeted glycolysis and oxidative

phosphorylation in overexpression models (HEK293T; Fig. 1A-D) and models of endogenous LRRK2 expression (primary astrocytes; Fig. 1E). HEK293T cells exogenously expressing WT LRRK2 were treated with the ATP-synthase inhibitor oligomycin or the mitochondrial uncoupling agent CCCP in glucose-free media. Both oligomycin and CCCP treatments induced a significant dephosphorylation of LRRK2 at S935 in the absence of glucose, but this was blocked in glucose-containing media (Fig. 1A, B). Oligomycin or CCCP treatment in glucose-free media induced depletion of intracellular ATP (Fig. 1C) while loss of mitochondrial membrane potential was only observed in CCCP conditions, as measured by high-content imaging and analysis of tetramethylrhodamine ethyl ester (TMRE) staining (Fig. 1D).

Oligomycin induced an increase in TMRE signal, suggesting hyperpolarization of the mitochondrial inner-membrane potential. We extended these data to examine rotenone, a complex I inhibitor that has been shown to modulate LRRK2 activity in different models (Di Maio, 2018). Rotenone treatment in glucose-free media induced dephosphorylation at S935 in a similar fashion to CCCP and oligomycin (see Supplementary Fig. S1A-C for additional mitochondrial toxin data). Lastly, we investigated the time course of LRRK2 dephosphorylation events under ATP-depletion. Dephosphorylation had plateaued at 45 min of ATP depletion while recovery of phosphorylation at S935 was achieved after 2 hrs in fresh glucose-containing media (Supplementary Fig. S1D, E). These data suggest that mitochondrial insults can affect S935 phosphorylation in glucose-deprived conditions and support a model whereby intracellular ATP levels modulate LRRK2 phosphorylation.

The effect of metabolic stress on LRRK2 phosphorylation was further validated in mouse primary cortical astrocytes that showed significant loss of endogenous pS935 under these conditions (Fig. 1E). Limiting the production of ATP from glycolysis and oxidative phosphorylation causes a shift in the intracellular AMP/ATP and ADP/ATP ratios resulting in phosphorylation and activation of AMPK (Moore et al., 1991; Stein et al., 2000). AMPK activation was verified by monitoring the increase in phosphorylation at T172 under oligomycin treatment. To validate these results in an ex vivo model, striatal sections were isolated from WT mice and incubated in glucose-free artificial cerebral spinal fluid (aCSF) supplemented with oligomycin, inducing the dephosphorylation of LRRK2 at S935 and S955 (Fig. 1F). The phosphatase PP1 has been identified as a regulator of LRRK2 constitutive phosphorylation (Lobbestael et al., 2013), thus we tested whether phosphatase inhibition can rescue dephosphorylation under metabolic stress. Calyculin A treatment inhibited the dephosphorylation of LRRK2 under metabolic stress in HEK293-T cells expressing WT LRRK2, at sites S910, S935, S955 and S973 (Fig. 1G). It is noteworthy that in the same metabolic stress conditions, AMPK (Garcia-Haro, 2010) which is an established PP1 substrate, is hyperphosphorylated (Fig. 1E). These data suggest that PP1 is not globally activated under metabolic stress, but instead its activity is regulated in a substrate-specific manner by distinct regulatory subunits (Casamayor and Ariño, 2020). To investigate the effect of metabolic stress on phosphorylation of LRRK2 genetic variants we looked at HEK293T cells transiently expressing LRRK2 mutants. Oligomycin treatment in glucose-free media induced the dephosphorylation of S935 in WT, R1441C, the kinase-dead variant K1906M, G2019S and S1292A (Supplementary Fig. S1F, G). Our data suggest that multiple forms of metabolic stress can induce a loss of constitutive LRRK2 phosphorylation via a mechanism that is largely independent of the kinase activity of the protein.

2.2. LRRK2 dephosphorylation is controlled by an AMPK-independent mechanism

AMPK is a metabolic regulator of cellular energy homeostasis. In conditions of low glucose, ischemia, hypoxia and heat shock, where intracellular ATP levels are depleted, AMPK is activated by binding to AMP, driving a metabolic shift toward processes that replenish cellular ATP (Hardie, 2011). AMPK is a heterotrimeric complex of a catalytic α

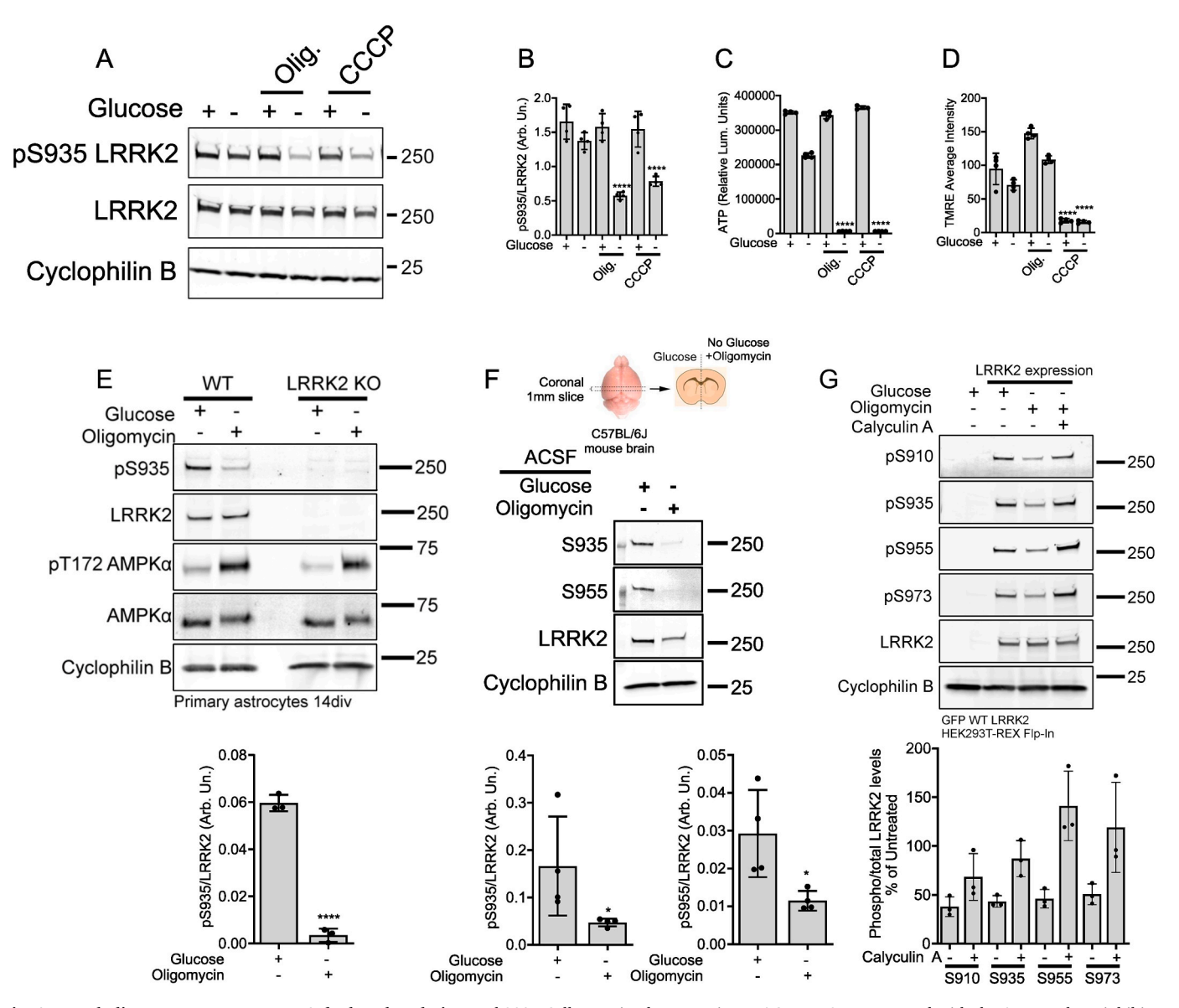


Fig. 1. Metabolic stress promotes LRRK2 dephosphorylation. Hek293T Cells transiently expressing FLAG LRRK2 were treated with the ATP synthase inhibitor oligomycin and the uncoupling agent CCCP in the presence or absence of glucose in culture. (A, B) In glucose-free media, oligomycin and CCCP induced LRRK2 S935 dephosphorylation. (C) ATP levels were depleted under oligomycin or CCCP treatment in the absence of glucose. (D) TMRE staining revealed depolarization of mitochondrial inner membrane potential by CCCP and hyperpolarization by oligomycin in the presence of glucose (one-way ANOVA; Tukey's post hoc test; ****p < 0.0001; n = 3 independent experiments). (E) Metabolic stress induced dephosphorylation of LRRK2 in primary mouse cortical astrocytes isolated from WT mice. Astrocytes from LRRK2 KO mice were analyzed alongside as a control for LRRK2 detection. (F) Ex vivo coronal slices were incubated in glucose-free aCSF in the presence of oligomycin inducing dephosphorylation of S935 and S955 LRRK2 (two-way ANOVA; n = 3 independent experiments; treatment: p < 0.0001, F(1,16) = 36.55; phosphosite: p = 0.04, F(3,16) = 3.490). (G) Treatment with the PP1 and PP2a inhibitor Calyculin A rescued dephosphorylation of LRRK2 under metabolic stress, in culture. (two-way ANOVA; Tukey's post hoc test; *p < 0.05; n = 3 independent experiments).

subunit and the regulatory β and γ subunits. A change in intracellular AMP:ATP ratio affects the binding of AMP to the γ subunit allosterically activating the complex and promoting phosphorylation at T172 in the activation loop of the α subunit by LKB1 (Hardie, 2011). To test whether AMPK activation under ATP depletion is necessary for the loss of constitutive LRRK2 phosphorylation at S935, LKB1 or different AMPK subunits were knocked-down by siRNA in cells stably expressing LRRK2. LKB1 knock-down did not rescue LRRK2 dephosphorylation under ATP depletion (Supplementary Fig. S2A). It is noteworthy that T172 phosphorylation of AMPK under ATP depletion was not inhibited by LKB1 knock-down suggesting that other kinases may be at play or/and low stoichiometric concentrations of LKB1 may still be sufficient to drive this phosphorylation event. In mammals there are seven genes encoding the subunits of the AMPK complex (Hardie, 2011). Partial knock-down of

the two α subunit isoforms $(\alpha 1,\,\alpha 2),$ and two isoforms of the β subunit $(\beta 1$ and $\beta 2)$ under ATP depletion did not rescue LRRK2 dephosphorylation (Supplementary Fig. S2B). Lastly, we examined whether pharmacological activation of AMPK is sufficient for LRRK2 dephosphorylation. AICAR, an AMPK activator, acts as an AMP analog within cells and binds to the γ subunit of AMPK inducing structural alterations in the enzyme. This facilitates the phosphorylation of the AMPK α subunit and AMPK activation (Sun et al., 2007). Treatment of cells with AICAR induced an increase in intracellular ATP levels through AMPK activation but this failed to modulate S935 phosphorylation (Supplementary Fig. S2C). Phosphorylation of acetyl-CoA carboxylase (ACC), an AMPK substrate, was assessed as a measure of AMPK activation. ACC phosphorylation was increased in glucose-free media and under AICAR treatment, but it was not followed by pS935

dephosphorylation. A decrease in pS935 levels was observed in ATP depleted cells in glucose-free media treated with CCCP or oligomycin. These data suggest that the loss of LRRK2 phosphorylation at S935 under metabolic stress takes place in a largely AMPK-independent mechanism.

2.3. Chronic 2-Deoxy-D-Glucose ingestion alters LRRK2 phosphorylation in vivo

2DG has a hydrogen at its C2 position instead of a hydroxyl group and cannot undergo glycolysis. It is internalized by cell surface glucose transporters and can be phosphorylated by hexokinase in the first step of glycolysis to produce 2-deoxyglucose 6-phosphate, which in turn competitively inhibits phosphoglucose isomerase blocking glycolysis. This compound has been put forward as a potential tool for dietary intervention to mimic calorie restriction in vivo (Ingram, 2006), as several lines of evidence suggest health benefits associated with calorie restriction in humans and animal models (Most et al., 2016). To recapitulate the effects of compromised energy production on LRRK2 in vivo, we looked at 2DG-fed rats that have been phenotypically and biochemically characterized previously (Minor et al., 2010). 3-Month old rats were fed regular chow supplemented with 0.6 %; 0.2 % or 0.04 % (w/w) 2DG for a 6 week period before collecting and analyzing the tissue (Minor et al., 2010). Phosphorylation of LRRK2 was analyzed in kidney and brain. In kidney, dephosphorylation of S935 was observed with increasing concentration of 2DG in the diet that reached significance at the 0.6 % (w/w) cohort (Supplementary Fig. S3A), while AMPK showed a marked increase in T172 phosphorylation in the high end of the 2DG concentration spectrum, recapitulating the metabolic effects of this treatment. In brain, S935 phosphorylated LRRK2 showed variability between groups and no significant difference when normalized to total LRRK2 protein (Supplementary Fig. S3B). AMPK T172 phosphorylation was largely unaltered in the brain tissue examined suggesting that the metabolic effects of 2DG ingestion were not seen in brain. This is in accordance with the original study that described these cohorts, whereby extensive pathology was only noted in heart and adrenal medulla (Minor et al., 2010). In cells, substituting glucose for 2DG induced a drop in intracellular ATP and LRRK2 dephosphorylation (Supplementary Fig. S4). These data cumulatively suggest that metabolic stress can modulate LRRK2 phosphorylation events and this can be recapitulated in various cellular and tissue models.

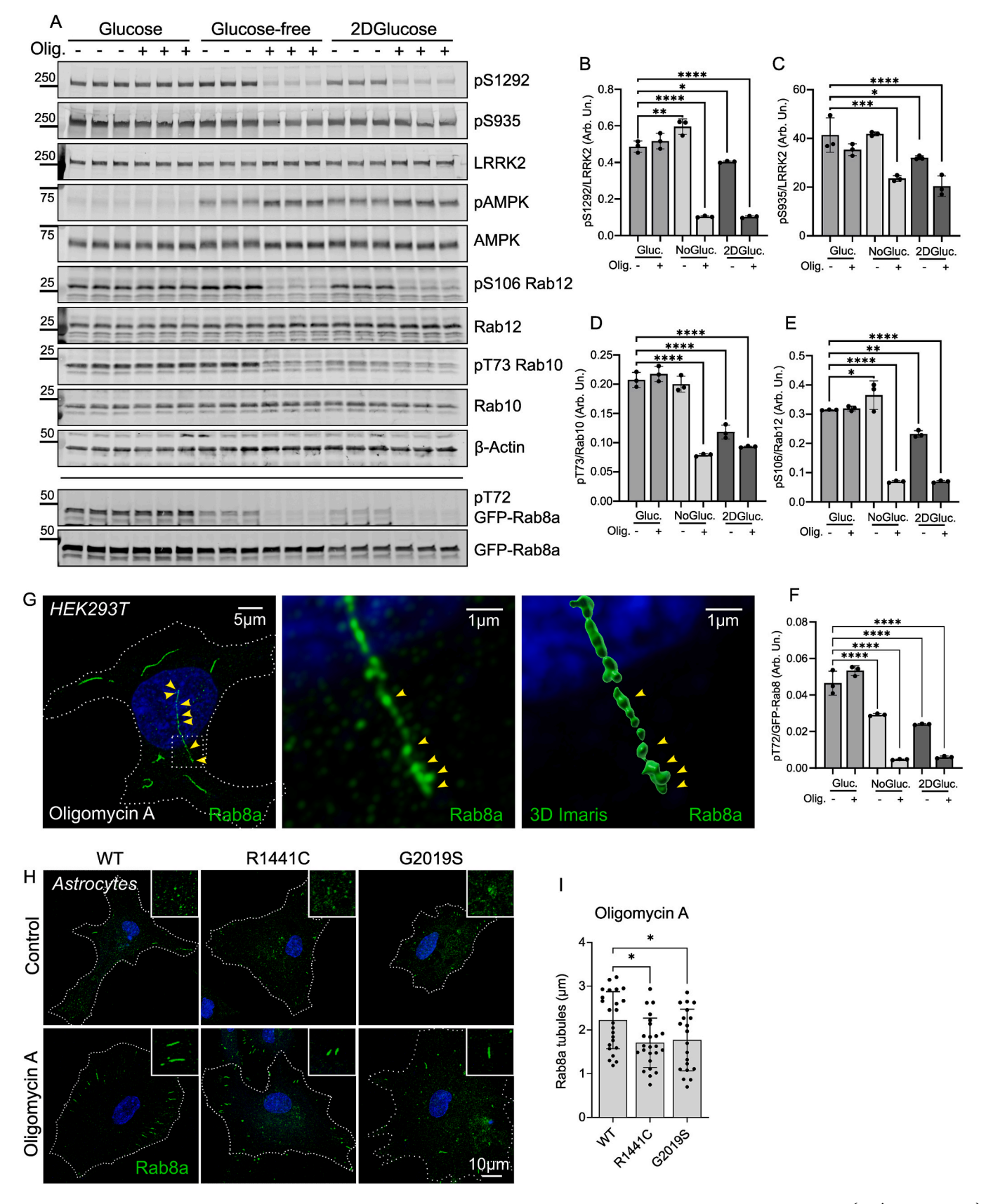
${\it 2.4. Metabolic stress modulates LRRK2 activity and Rab8a localization in cells}$

S910/S935 phosphorylation status affects LRRK2 binding to 14-3-3 proteins and this can modulate LRRK2 localization and activity (Nichols et al., 2010). Structural studies show that 14-3-3 binding maintains LRRK2 in an autoinhibited state, while loss of S910/S935 phosphorylation and 14-3-3 interaction activates LRRK2 (Martinez Fiesco, et al., 2024). 14-3-3 can inhibit the function of GTP-binding Rnd proteins by trapping them in the cytosol (Riou et al., 2013), suggesting that 14-3-3 binding might alter LRRK2 interactome. PD-linked mutations in the Roc/COR bidomain affect S910/S935 phosphorylation while increasing the kinase activity of LRRK2 towards Rab GTPase substrates (Steger, et al., 2016). S935 phosphorylation can be induced by inflammatory stimuli while studies employing phospho-null mutants show that S935 phosphorylation status can modulate macroautophagy and the kinase activity of the protein towards Rab GTPases (Kania, 2023). To explore whether modulation of constitutive phosphorylation by metabolic stress is accompanied by changes in kinase activity, cells stably expressing exogenous LRRK2 were treated with oligomycin in standard glucose media, glucose-free media or glucose-free media supplemented with 2DG and autophosphorylation and Rab GTPase phosphorylation were assayed by Western blot (Fig. 2). Glucose starvation increased LRRK2 autophosphorylation along with pS106 Rab12 but not T73 Rab10 phosphorylation while acute oligomycin treatment in glucosefree media attenuated LRRK2 activity (Fig. 2A-E). 2DG with or without oligomycin led to a significant dephosphorylation of S1292 and S935 LRRK2, Rab12 and Rab10. To assess Rab8a phosphorylation, we exogenously expressed GFP Rab8a, as the only available pT72 Rab8a antibody at this time (ab230260) lacks specificity and cross-reacts with other Rab GTPases which migrate at ~24 kDa. By using a GFP-tagged construct, we were able to distinguish Rab8a from other endogenous Rabs on immunoblots. Glucose deprivation led to decreased Rab8a phosphorylation, contrasting with the regulation observed for Rab10 and Rab12 (Fig. 2A, F). The divergent response of Rab8a compared to Rab10 and Rab12 may indicate compartment-specific regulation and energy dependence of Rab8a-pathways, prompting us to next examine how metabolic stress impacts Rab8a's localization and function at the endocytic recycling compartment.

The endocytic recycling compartment (ERC) is a specialized intracellular structure involved in the sorting and recycling of endocytosed cargo and receptors back to the plasma membrane. Tubular recycling endosomes are elongated, tubule-like structures that form part of the ERC. We, and others, have shown that Rab8a localizes on tubular endosomes where it can mediate cargo sorting and recycling of receptors (Kobayashi et al., 2014; Sharma et al., 2009; Mamais et al., 2021). In turn, mutant LRRK2 hyperphosphorylates Rab8a affecting its localization and function (Steger, et al., 2016; Mamais et al., 2021; Madero-Pérez et al., 2018). Rab8a is involved in the formation and maintenance of the tubular structure of endosomes facilitating elongation of endosomal tubules and efficient cargo transport. Lastly, ATP hydrolysis is important for membrane remodeling and endosomal tubule scission (Deo, 2018). To investigate how metabolic stress and LRRK2 mutations can affect Rab8a association with tubular endosomes we treated cells with oligomycin in glucose-free media and stained for endogenous Rab8a. Rab8a localized in recycling endosomes and tubular structures in control cells while metabolic stress significantly induced Rab8a tubule formation (Supplementary Fig. S5). Super-resolution microscopy revealed the formation of beaded structures indicating impaired endosomal scission as previously described (Wunderley, 2021) (Fig. 2G). We quantified the maximum length of Rab8a tubular endosomes in mouse primary astrocytes under metabolic stress and found shortening of these structures in cells homozygous for G2019S and R1441C mutations (Fig. 2H, I). Our data suggest that LRRK2 mutations affect Rab8apositive tubular endosome dynamics under metabolic stress.

2.5. Manganese exposure activates LRRK2 in cells

As an orthogonal approach to understand the role of environmental toxic exposure in LRRK2 activation, we aimed at inducing cellular stress through exposure to excess manganese, a heavy metal implicated in the etiology of PD. Manganese is an essential trace element involved in distinct biological processes, but excessive levels can be toxic, particularly to mitochondria. Excessive manganese can lead to significant mitochondrial dysfunction through oxidative stress, disruption of the electron transport chain, impaired calcium homeostasis, and induction of apoptosis (Diessl, 2022; Harischandra, 2019; Smith et al., 2017). These effects are particularly relevant in neurotoxicity associated with PD. Chronic exposure to manganese is known to cause manganism, a neurodegenerative condition resembling PD (Harischandra, 2019). Manganese-induced mitochondrial dysfunction in the brain can lead to cognitive deficits and motor impairments. Recently, manganese exposure was nominated as an activator of LRRK2 kinase (Kim, 2019) and it has been previously reported that mutant G2019S LRRK2, but not WT LRRK2, can utilize manganese instead of MgCl2 as the metal co-factor in its kinase function (Covy and Giasson, 2010). Here, we assayed the modulation of LRRK2 phosphorylation and activity by manganese exposure. Cells expressing exogenous LRRK2 were treated with 100 μM manganese in culture overnight prior to collection and analysis. Manganese treatment induced S1292 LRRK2 autophosphorylation along with T73 Rab10 and S106 Rab12 phosphorylation, while these effects



(caption on next page)

Fig. 2. Metabolic stress modulates LRRK2 kinase activity. (A) Cells expressing GFP LRRK2 were acutely treated with oligomycin following incubation in media containing glucose, 2DG or glucose-free and LRRK2 phosphorylation and activity were assessed. (B) LRRK2 autophosphorylation was increased following glucose deprivation, while 2DG alone or co-treatment with oligomycin abolished kinase activity. (C-F) Culturing in 2DG-containing media or treatment with oligomycin in glucose-free media reduced pS935 LRRK2 levels as well phosphorylation of Rab10, Rab12 and GFP Rab8a. (E, F) Rab12 phosphorylation at S106 was increased while GFP Rab8a phosphorylation at T72 was decreased with glucose starvation (one-way ANOVA; Tukey's post hoc test; *p < 0.05, **p < 0.01, ***p < 0.001, ****p < 0.0001; n = 3 independent replicates). (G) HEK293T cells were treated with oligomycin in glucose-free media and endogenous Rab8a was stained, revealing the formation of Rab8a-positive tubules part of the ERC. Super-resolution confocal microscopy revealed elongation of Rab8a-positive beaded tubules following metabolic stress, visualized by 3D rendering on the Imaris platform. (H) Primary astrocytes isolated from WT, R1441C homozygous and G2019S homozygous mice were treated with oligomycin in glucose-free media and Rab8a was stained and imaged. (I) Mutant LRRK2 astrocytes exhibited shorter Rab8a-positive tubules under metabolic stress (one-way ANOVA; Tukey's post hoc test; *p < 0.05; n > 20 cells from two independent experiments).

were reversed by acute MLi-2 treatment (Fig. 3A-E). Interestingly, pS935 levels were decreased by manganese treatment mimicking metabolic stressors as described before (Fig. 3C).

We, and others, have shown that LRRK2 activity is intrinsically linked to its dimerization (Mamais et al., 2014; Berger et al., 2010). We examined the dimerization and activity of LRRK2 following manganese exposure in culture. Exposure to manganese, even at high concentrations, did not significantly alter LRRK2 dimerization or total levels (Fig. 3H, I). As LRRK2 kinase activity is linked to its dimerization, we examined the intrinsic kinase activity of purified dimers following exposure of cells to manganese. We performed an in vitro kinase reaction on captured dimeric LRRK2 using the NICtide peptide substrate (Leandrou et al., 2019). Exposure to manganese caused a dosedependent increase in the intrinsic kinase activity of purified LRRK2 dimers, compared to LRRK2 dimers from untreated cells (Fig. 3J). Without evident changes in total LRRK2 expression or its dimerization induced by manganese exposure, this raises the possibility of additional post-translational modifications in LRRK2. Lastly, we validated these data by assessing pT73 Rab10 levels by immunofluorescence. Endogenous pT73 Rab10 intensity was increased in cells expressing LRRK2 in conditions of manganese overload in culture while this was reversed by MLi-2 treatment (Fig. 3K, L). Our data validate manganese-induced metabolic stress playing a role in the activation of LRRK2 and highlight parallel but distinct pathways of LRRK2 phospho-modulation by metabolic insults.

2.6. Time course shows distinct kinetics for LRRK2, Rab10 and Rab12 phosphorylation under manganese exposure

To dissect the temporal dynamics of LRRK2 activation following manganese exposure, we conducted a time-course experiment in FLAG LRRK2 expressing HEK293T cells treated with 100 µM MnCl₂ for 30 min to 24 h. LRRK2 autophosphorylation at S1292 was increased by 30 min and peaked at 6 h, consistent with previous reports linking metalinduced oxidative stress to heightened LRRK2 activity (Kim, 2019; Lovitt et al., 2010) (Fig. 4A, B). In parallel, phosphorylation at S935 showed a trend toward an increase following 1 hr treatment but significantly decreased over time at later time-points, highlighting a dissociation between constitutive and kinase-associated phosphorylation sites. Strikingly, Rab GTPase substrates exhibited markedly different phosphorylation kinetics. Rab12 phosphorylation at S106 was strongly induced by 30 min of Mn exposure, suggesting it may be an early and sensitive substrate of LRRK2 in stress conditions. By contrast, Rab10 phosphorylation at T73 was delayed, with levels gradually increasing and peaking only after 24 h. This divergence in substrate kinetics aligns with prior observations that Rab10 and Rab12 differ in their recruitment dynamics and subcellular targeting following LRRK2 activation (Steger, et al., 2016; Kania, 2023). Co-treatment with the selective LRRK2 kinase inhibitor MLi-2 during the final two hours abolished phosphorylation of both Rab GTPases, confirming that these effects were LRRK2-dependent. These results reveal that manganese triggers a sequential activation of LRRK2 signaling, with substratespecific temporal profiles that may reflect differences in subcellular accessibility or phosphatase turnover (Fig. 4).

2.7. Phosphorylated Rab10 localizes to centrosomes and lysosomes following manganese exposure

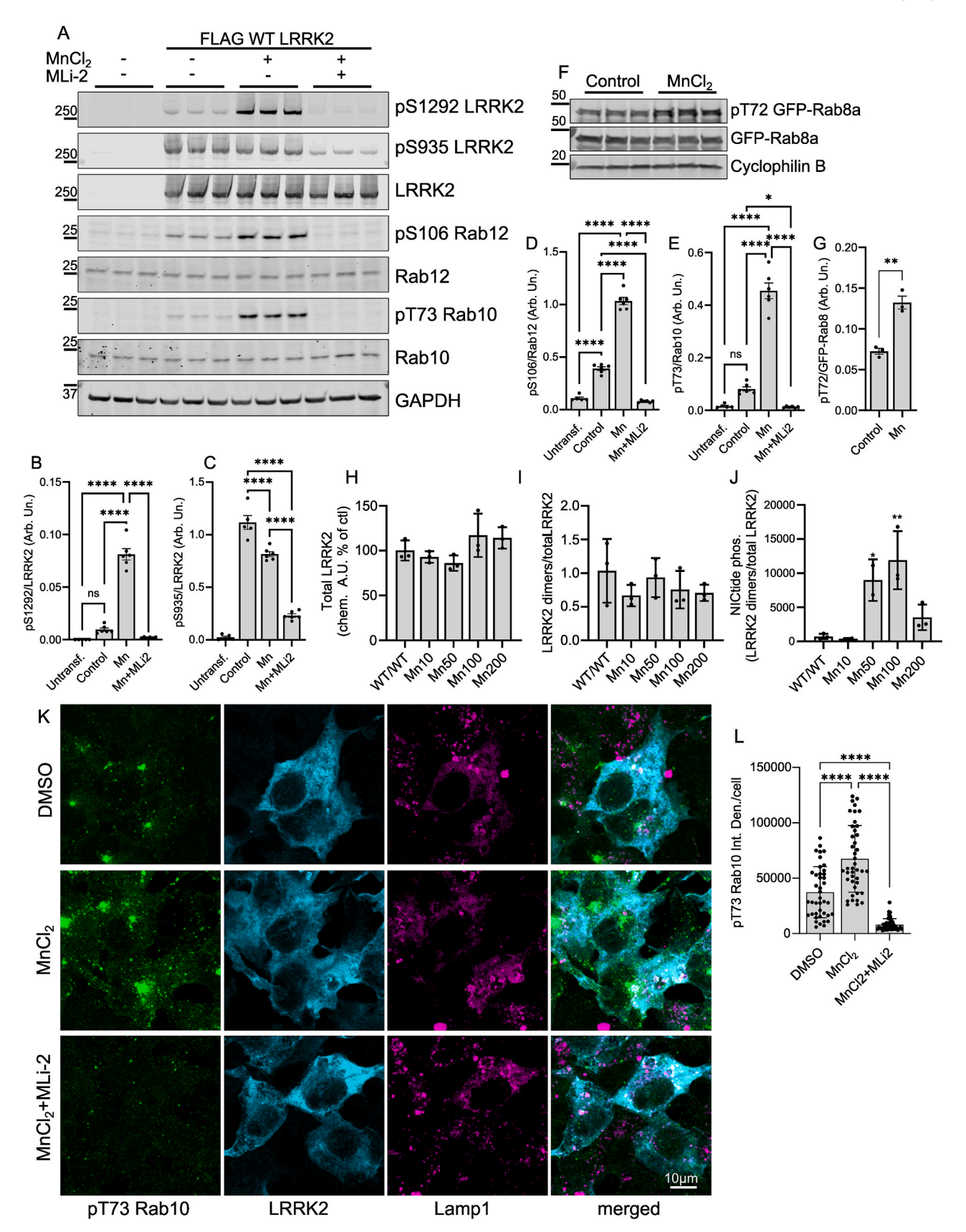
We, and others, have shown that LRRK2 is activated and phosphorylates Rab10 at the lysosome, in response to lysosomal damage (Bonet-Ponce, et al., 2020; Eguchi, 2018). Given the robust induction of Rab10 phosphorylation by manganese, we next examined its subcellular localization in cells expressing WT LRRK2 following MnCl₂ exposure. Immunostaining revealed a striking accumulation of pT73 Rab10 at both centrosomes and lysosomes after overnight treatment, as revealed by increased colocalization with pericentrin and Lamp2 (Fig. 5A, B). These data indicate that LRRK2 activation under manganese stress remains closely associated with both lysosomal and centrosomal compartments.

2.8. Manganese impairs mitochondrial respiration and promotes ROS-dependent LRRK2 activation

Given the convergence of metabolic stress and manganese exposure on LRRK2 signaling, we next sought to compare their downstream effects on mitochondrial function and oxidative stress. In prior work, we and others have shown that ROS can activate LRRK2 kinase activity and modulate its subcellular localization (Di Maio, 2018; Mamais et al., 2014; Keeney, 2024), prompting us to investigate whether manganese, a known inducer of mitochondrial ROS (Smith et al., 2017; Morcillo et al., 2021; Fernandes, 2017; Rao and Norenberg, 2004), acts through a similar mechanism. Using Seahorse XF extracellular flux analysis, we found that MnCl2 treatment caused a broad impairment of mitochondrial bioenergetics, decreasing basal and maximal respiration as well as ATP-linked oxygen consumption rate (OCR) (Fig. 6A-H). Defects in mitochondrial respiration were observed independently of extracellular glucose availability, underscoring that manganese induces a targeted defect in mitochondrial respiration. In parallel, manganese exposure elevated intracellular ROS, modestly depolarized the mitochondrial membrane potential, and lowered cellular ATP (Fig. 6I-K), consistent with the energetic failure observed under metabolic stress. To directly test whether ROS mediates LRRK2 activation in this context, we cotreated cells with the antioxidant N-acetylcysteine (NAC). Strikingly, NAC rescued pT73 Rab10 phosphorylation in manganese-treated cells, indicating that redox imbalance is a key upstream driver of LRRK2 activity under manganese stress (Fig. 6L, M). These findings underscore a mechanistic link between mitochondrial dysfunction, oxidative stress, and LRRK2 activation, and establish a shared pathway connecting metabolic and environmental insults in the regulation of LRRK2 signaling.

3. Discussion

Soon after the identification of LRRK2 as a PD gene, early studies reported that the kinase activity of the protein was enhanced by pathologic mutations and this was likely driving disease (Greggio, 2006). Mutations in LRRK2 may increase the kinase activity of the protein through various biochemical mechanisms including augmented kinase activity dynamics, altered substrate specificity, and decreased GTPase activity (Biosa, 2013; Lewis et al., 2007; Schmidt et al., 2019). While increase of LRRK2 kinase activity through mutations is linked to familial



(caption on next page)

Fig. 3. Manganese exposure activates LRRK2 in culture. Cells transiently expressing FLAG LRRK2 were treated overnight with 100 μM MnCl₂ in culture followed by a 1hr MLi-2 treatment to test rescue. (A) Mn treatment induced S1292 phosphorylation but decreased phosphorylation at S935 (B, C). (D, E) Mn treatment induced phosphorylation of Rab10 and Rab12 while these effects were reversed by MLi-2 treatment. (B-E; one-way ANOVA, Tukey's post hoc test; n = 6 replicates across two independent experiments; ****p < 0.0001; *p < 0.05). (F, G) Cells transiently expressing FLAG LRRK2 and GFP Rab8a were treated overnight with 100 μM MnCl₂ in culture prior to collection and analysis. Manganese treatm7ent induced phosphorylation of GFP Rab8a at T72 (G; student *t*-test; n = 3 biological replicates, **p < 0.01). (H-J) Hek293T cells expressing WT/WT LRRK2 proximity biotinylation constructs were exposed to increasing concentrations of Mn. Cell extracts were processed to quantify total and dimeric LRRK2 as well as the intrinsic activity of the isolated dimers. (H, I) Increasing concentrations of Mn did not alter dimer formation, but the intrinsic kinase activity of the isolated dimers was increased (J). (K, L) Hek293T cells transiently expressing FLAG LRRK2 were treated with MnCl₂ overnight and pT73 Rab10 was assessed by staining, validating increase in Rab10 phosphorylation that was rescued by MLi-2 treatment (one-way ANOVA, Tukey's post hoc test; n > 40 cells from two independent experiments; ****p < 0.0001).

PD, levels of LRRK2 protein and activation of the WT protein are linked to idiopathic PD progression (Di Maio, 2018; Cook, 2017) and also implicated in monogenic forms of the disease linked to other PD genes (Mir et al., 2018; Bu, 2023; Gustavsson, 2024), highlighting the need to understand the physiological triggers that activate WT LRRK2 protein. We, and others, have reported cellular triggers that modulate LRRK2 in different systems, including oxidative stress (Di Maio, 2018; Mamais et al., 2014), lysosomal damage (Bonet-Ponce, et al., 2020; Eguchi, 2018) and inflammation (Dzamko, 2012). While different lines of evidence have highlighted pathways of LRRK2 activation in overexpression models, what is lacking is an understanding of how different metabolic stressors can modulate endogenous LRRK2. We set out to answer this by employing metabolic stressors and heavy metal exposure in cellular and ex vivo models with established readouts of LRRK2 phosphorylation and activity. We observed a decrease in S935 phosphorylation in conditions when both glycolysis and oxidative phosphorylation were inhibited and concomitant loss of Rab GTPase phosphorylation reflecting LRRK2 inhibition. Glucose deprivation in cells induced a mild increase in LRRK2 kinase activity while this was not recapitulated by 2DG treatment in culture. Lastly, manganese exposure in cultured cells had a similar effect with pS935 loss but a striking dose-dependent activation of LRRK2 that was rescued by antioxidants, and a divergence in the kinetics of Rab10 and Rab12 phosphorylation. Our working model is that metabolic stress leading to ATP depletion suppresses LRRK2 activity, whereas mitochondrial stress resulting in ROS production through manganese exposure promotes LRRK2 activation. Our data link different modalities of environmental stressors and age-related processes to physiological modulation of LRRK2 activity (Fig. 7).

Cellular stress is thought to play a significant role in the development of PD, with genes linked to the condition, such as PARK2, PINK1, and DJ1, being connected to mitochondrial dysfunction and increased cellular effects related to ROS. The characteristic loss of dopaminergic cells in PD can be replicated in vivo through exposure to toxins like MPTP or rotenone, which inhibit Complex I of the mitochondrial respiratory chain. In addition to mitochondrial dysfunction, mutant LRRK2 has also been shown to promote endoplasmic reticulum stress, further implicating its role in cellular vulnerability and PD pathogenesis (Yao, 2023). LRRK2 has been associated with protection against mitochondrial stress by interacting with kinases of the mitogen-activated protein kinase family, while studies indicate that the G2019S mutation in LRRK2 leads to the uncoupling of mitochondrial oxidative phosphorylation (Papkovskaia et al., 2012) and impairment of canonical pathways driving reduction in the antioxidant response and increased ROS (Kim, 2023). More importantly, recent evidence suggests that oxidative stress can modulate LRRK2 activity. In cells, H2O2 treatment activates LRRK2 kinase as measured by pS1292 and Rab10 phosphorylation using a proximity ligation assay (Di Maio, 2018). In contrast, a separate study showed that oxidizing agents can lead to LRRK2 inactivation through oxidation of a unique pair of adjacent cysteines in LRRK2 (Trilling, 2024). Our earlier work has also placed LRRK2 in metabolic signaling with its kinase activity downregulated by arsenite treatment that can affect different aspects of cellular energy production (Mamais et al., 2014). Here, we explored how specific mitochondrial toxins may affect LRRK2. We show that inhibiting mitochondrial respiration by oligomycin, which inhibits the ATP synthase complex residing in the inner

mitochondrial membrane (Pagliarani et al., 2013), CCCP, a mitochondrial uncoupler, or rotenone did not affect LRRK2 constitutive phosphorylation in glucose-rich media. In contrast, all mitochondrial toxins tested induced S935 dephosphorylation in glucose-free media. This suggests that inhibiting mitochondrial function is required but not sufficient to modulate S935 phosphorylation in cells under glucose deprivation conditions.

LRRK2 activity has been the focus of extensive research since it is augmented by PD-linked mutations and thus kinase inhibitors have been developed as possible therapeutic means. S935 phosphorylation has been used as a proxy readout for kinase activity in clinical trials of LRRK2 inhibitors, even though the mechanism by which LRRK2 kinase inhibition feeds back to S935 dephosphorylation is not fully elucidated. Recent structural and biochemical studies show that Type I inhibitors, which bind the active kinase conformation, promote S935 dephosphorylation by inducing conformational changes that destabilize 14-3-3 protein binding and expose the site to phosphatases. In contrast, Type II inhibitors, which bind the inactive conformation, preserve S935 phosphorylation despite effectively inhibiting kinase activity, suggesting that S935 status is not a direct indicator of catalytic inhibition but reflects changes in LRRK2 folding and complex formation (Tasegian et al., 2021; Raig, et al., 2024). Cryo-electron microscopy has revealed that LRRK2 forms an autoinhibited complex with a 14-3-3 protein dimer that binds phosphorylated residues S910 and S935, stabilizing an inactive monomeric state by limiting LRR domain flexibility and preventing its dimerization (Martinez Fiesco, et al., 2024). Loss of constitutive phosphorylation, thus, releases the autoinhibitory state activating the kinase (Martinez Fiesco, et al., 2024). In fact, quadruple LRRK2 phospho-null cells (S910A/S935A/S955A/S973A) show impaired lysosomal integrity and starvation-induced autophagy mediated through enhanced LRRK2 kinase activity (Kania, 2023). Here, we show that short-term glucose deprivation was adequate to activate LRRK2 in cultured cells reflected by increased S1292 LRRK2 and S106 Rab12 phosphorylation. Cellular stress by glucose deprivation can induce autophagy (Choi et al., 2015) and recent data suggest that starvation in HBSS can induce LRRK2 constitutive phosphorylation in cells (Kania, 2023). These data are consistent with rapamycin-induced macroautophagy stimulating indices of LRRK2 activity in cells (Schapansky et al., 2014). Macroautophagy is believed to be activated through activation of AMPK that phosphorylates Ulk1, to supply energy to glucose-deprived cells as a cell survival mechanism (Kim et al., 2011). This would support the hypothesis that glucose deprivation can induce LRRK2 activity through autophagic signaling. It is noteworthy, however, that 2DG treatment induced LRRK2 inactivation in cells. This may be driven by the fact that autophagy itself is energy-intensive, involving membrane reorganization and transport. In fact, a recent study showed that blocking glycolysis can suppress amino acid starvation-induced stimulation of Ulk1 signaling via AMPK activation and inhibit autophagy (Park et al., 2023). Thus, in cells lacking glucose, the initiation of autophagy may rely on their capacity to access a baseline level of energy that is blocked by 2DG. In our experiments, glucose deprivation did not substantially lower cellular ATP levels while 2DG did, suggesting that low ATP levels may interfere with autophagy related activation of LRRK2.

Calorie restriction has been modeled *in vivo* by the glucose analog 2DG, that inhibits glycolysis and simulates a state of reduced glucose

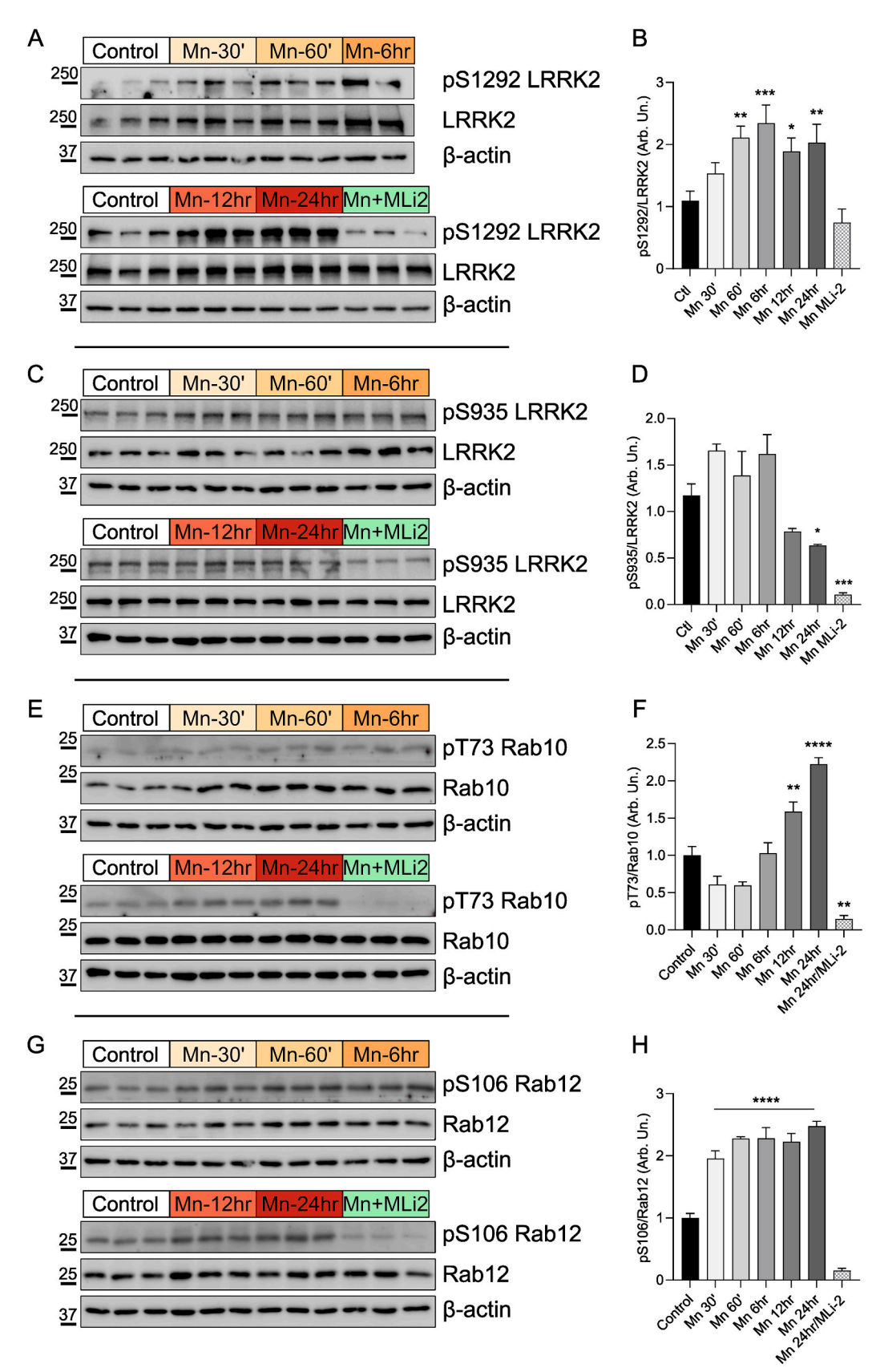


Fig. 4. Time-course of LRRK2 activation by manganese exposure. Cells transiently expressing FLAG LRRK2 were treated with $100 \mu M$ MnCl₂ in culture for 30 mins, 60 mins, 60 mins, 6 hrs, 12hrs and 24hrs as well as co-treated with Mli-2 for the last 2 hrs prior to collection. LRRK2 pS1292 autophosphorylation peaked at 6 hrs while a biphasic regulation in pS935 was noted with significant reduction at 24 hrs. Interestingly, pS106 Rab12 was maximally phosphorylated by 30 mins exposure to manganese in culture while pT73 Rab10 showed a much slower phosphorylation peaking at 24 hrs treatment (one-way ANOVA; Tukey's post hoc test; *p < 0.05, **p < 0.01, ***p < 0.001, ***p < 0.001; n = 6 replicates across two independent experiments).

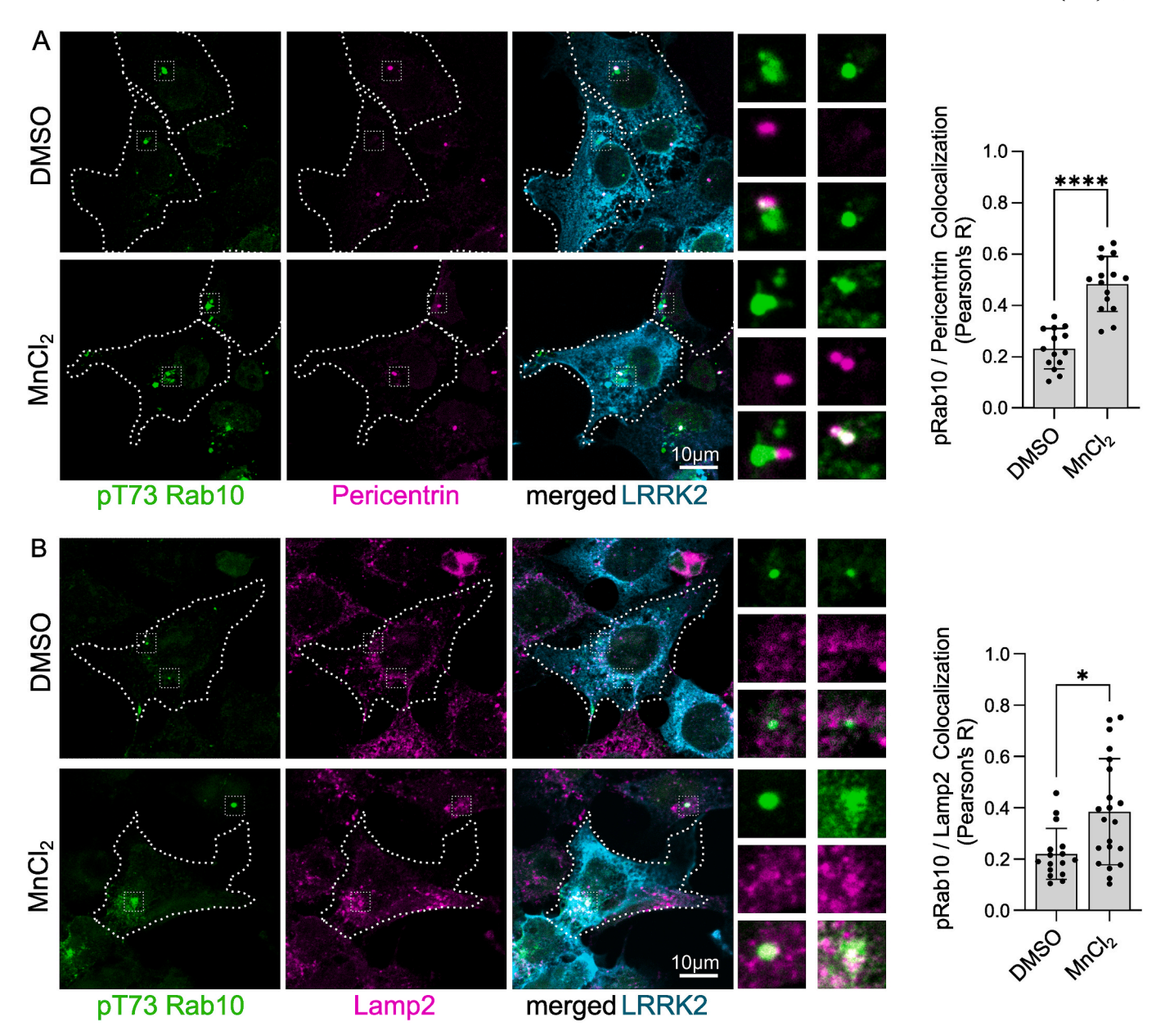


Fig. 5. Manganese exposure promotes Rab10 phosphorylation and association with centrosomes and lysosomes. Cells transiently expressing FLAG LRRK2 were treated overnight with $100 \mu M$ MnCl₂ in culture and stained for pT73 Rab10, Lamp2, Pericentrin and LRRK2. Mn treatment induced colocalization of pT73 Rab10 with pericentrin (A) and Lamp2 (B) revealing increased association with centrosomes and lysosomes (student t test; n > 15 cells from two independent experiments; *p < 0.05; ****p < 0.0001).

availability. A number of cellular pathways are affected by 2DG that drive energy production, metabolic pathways and cellular stress responses. Autophagy and autophagic flux is reportedly activated in the chronic calorie restriction by 2DG ingestion cohort analyzed here (Minor et al., 2010). AMPK is an energy-sensing kinase that regulates metabolic pathways to regulate energy homeostasis and it is activated by increased AMP/ATP or ADP/ATP ratios (Sun et al., 2007; Ke et al., 2018). Activating AMPK pharmacologically failed to modulate LRRK2 phosphorylation in culture while an increase in ATP was noted. This suggests that while AMPK activation is not sufficient to induce S935 dephosphorylation, calorie restriction was an accurate predictor of loss of constitutive LRRK2 phosphorylation in cells and in vivo. Interestingly, metabolic risk factors, including fasting blood glucose, affect the success of deep brain stimulation in patients (Yao, 2025). A recent study showed that dietary influences on protein synthesis and autophagy are critical determinants of neurodegeneration in a Drosophila model of LRRK2 PD

(Chittoor-Vinod, 2020). Our work suggests that calorie restriction is a modulator of LRRK2 activity and whether this plays a role in the pathogenic effect of LRRK2 warrants further investigation.

Our data suggest that LRRK2 mutations can affect Rab8a tubular recycling endosome length in primary astrocytes under metabolic stress. Rab8a plays a key role in regulating membrane dynamics and cellular trafficking pathways and LRRK2 mutations have been reported to affect Rab8a functions (Pfeffer, 2023; Mamais et al., 2021; Madero-Pérez et al., 2018). We have shown that Rab8a localizes on tubular endosomes and LRRK2 mutations sequester Rab8a and other ERC factors to damaged lysosomes while impairing TfR1 recycling (Mamais et al., 2021). Rab8a is a key regulator of polarized membrane trafficking and tubular recycling endosomes, playing an essential role in the recycling of surface receptors such as TfR1 and glucose transporter 1 (GLUT1) (Li et al., 2017; Burtey, 2015; Ang, 2004; Hattula, 2006). In the CNS, Rab8a-mediated trafficking supports neurite outgrowth (Homma and Fukuda,

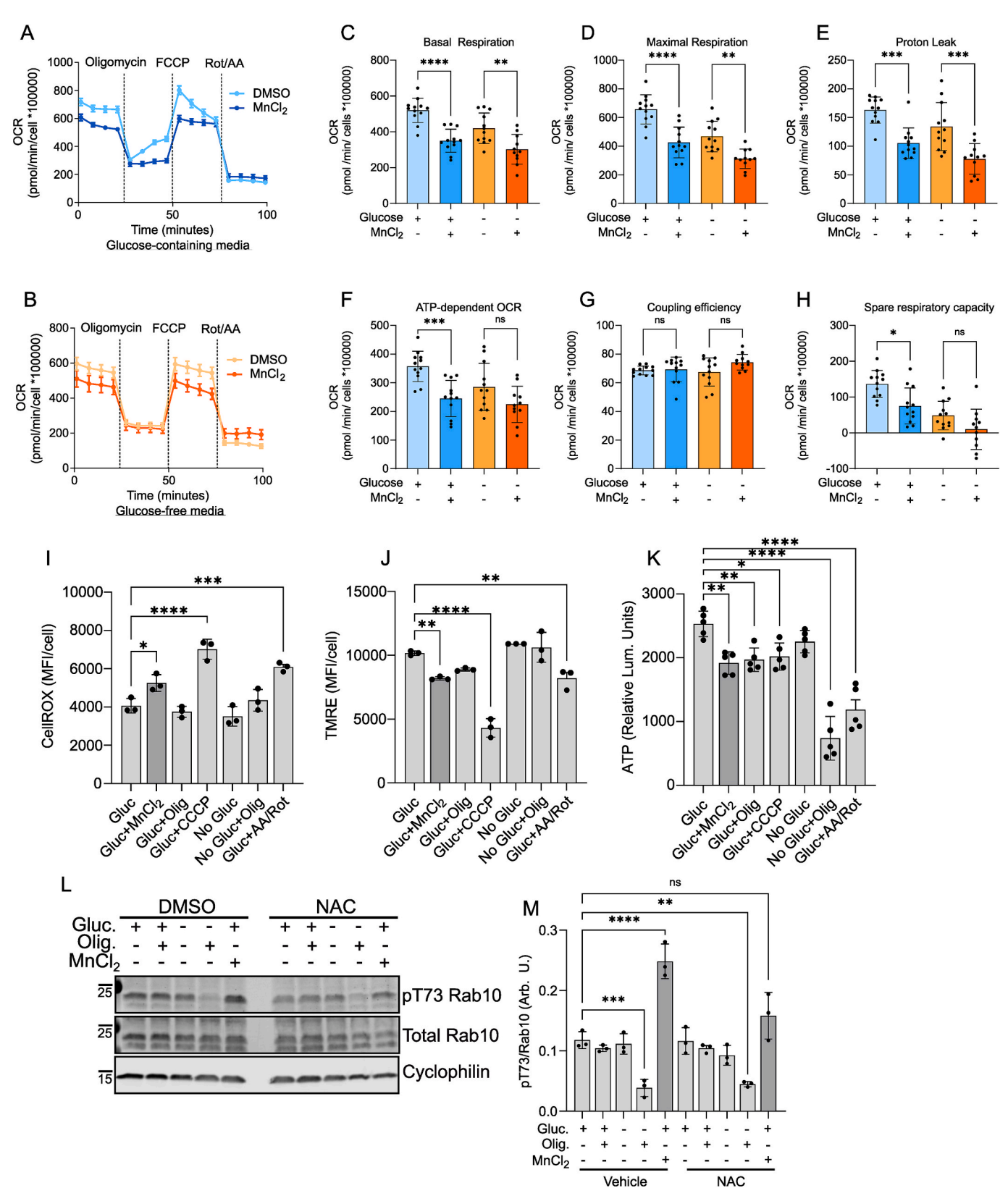


Fig. 6. Manganese exposure compromises mitochondrial function and induces ROS-dependent Rab10 phosphorylation. Cells were treated with $MnCl_2$ and mitochondrial respiration parameters were assessed using Seahorse XF analysis. Manganese treatment caused global mitochondrial function impairment affecting basal and maximal respiration as well as ATP-dependent respiration, independent of glucose in the media (A-H). Manganese exposure induced ROS, mild mitochondrial membrane depolarization and a decrease in cellular ATP (I, J, K). Cells expressing LRRK2 were treated with $MnCl_2$ in the presence or absence of N-acetylcysteine (NAC). Antioxidant treatment rescued Rab10 phosphorylation by LRRK2 under manganese exposure. (one-way ANOVA, Tukey's post hoc test; n=3 independent replicates; *p < 0.05; **p < 0.01; ***p < 0.001; ****p < 0.0001).

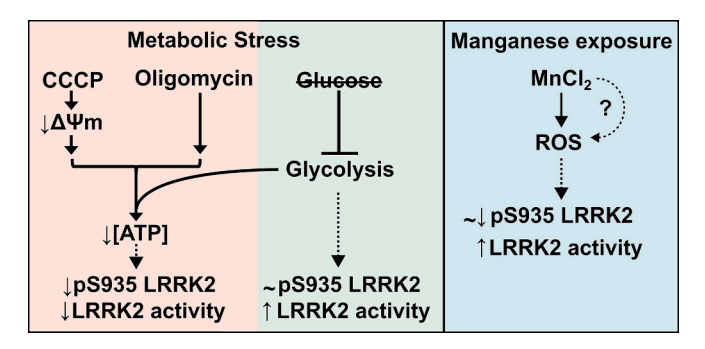


Fig. 7. A model of the modulation of LRRK2 by metabolic stress and heavy metal exposure. Inhibition of mitochondrial function in glucose-free media that results in ATP depletion induces loss of constitutive LRRK2 phosphorylation and inhibition of its kinase activity while glucose deprivation alone activates LRRK2 kinase. Mitochondrial stress resulting in ROS through manganese exposure induces LRRK2 activity.

2016), modulates metabotropic glutamate receptor trafficking (Esseltine et al., 2012) and mediates the delivery and recycling of AMPA receptors, important for synaptic transmission (Hattula, 2006; Brown et al., 2007). Furthermore, Rab8 can modulate Toll-like Receptor signaling and mediates trafficking of surface proteins involved in astrogliosis (Schiweck et al., 2021; Wall, 2017). The shortening of Rab8a-positive tubules we observe in LRRK2 mutant astrocytes likely reflects a defect in the formation or stability of tubular carriers, which may impair the delivery of cargo to the plasma membrane (Yoshimura et al., 2007). This is particularly relevant in PD, where altered astrocyte function can contribute to dopaminergic vulnerability (Booth et al., 2017). Our recent work demonstrated that genetic inactivation of Rab8a in human neurons results in increased α-synuclein accumulation, altered lysosomal pH, and disrupted Golgi organization (Mamais et al., 2024), hallmarks of PD cellular pathology. Given Rab8a's essential role in trafficking and maintenance of endolysosomal homeostasis, the loss of tubule integrity likely reflects impaired membrane extension and sorting capacity, which can disrupt astrocytic support for neurons. In glia, this could lead to defective recycling of transferrin and glucose transporters, as well as impaired clearance of extracellular α -synuclein. It is noteworthy that our data point to tubular endosome alterations in metabolic stress conditions when LRRK2 is inactivated, as demonstrated by loss of autophosphorylation and phosphorylation of Rab GTPases. These findings suggest that LRRK2 mutations may perturb Rab8a-dependent trafficking in astrocytes, revealing a potentially underexplored mechanism linking vesicle dynamics to non-cell-autonomous mechanisms of PD progression.

Manganese has been implicated in PD through epidemiological, genetic and functional studies. Manganese induces ROS and impairs mitochondrial function through oxidative stress and disruption of the electron transport chain (Smith et al., 2017; Morcillo et al., 2021; Fernandes, 2017; Rao and Norenberg, 2004). Mutations in SLC30A10, a cell surface protein involved in the efflux of manganese, lead to manganese accumulation and parkinsonian-like syndromes (Quadri et al., 2012). In a chronic exposure setting, manganese accumulates mainly in the basal ganglia and leads to manganism, a syndrome that resembles PD with symptoms of cognitive dysfunction and motor impairment (Harischandra, 2019; Peres et al., 2016). Recent studies have reported a role for LRRK2 in manganese-induced cytotoxicity and inflammation in microglial cells and mouse models, through phosphorylation of Rab10 (Kim, 2019; Chen et al., 2018; Pajarillo et al., 2023). In fact, early studies showed that G2019S LRRK2 kinase is activated by manganese, in vitro (Lovitt et al., 2010). Our data showing LRRK2 activation by manganese in culture are in accordance with earlier studies linking LRRK2 activity with manganese. Interestingly, we observed increased association of pRab10 with the centrosome and lysosome following manganese-driven LRRK2 activation. The centrosomal accumulation of pRab10 echoes

previous observations in LRRK2 mutant models where Rab phosphorylation at the pericentriolar region disrupts centrosomal cohesion and ciliogenesis (Lara Ordónez, 2019; Dhekne, 2018). Moreover, lysosomal localization of LRRK2 substrates has been documented in the context of lysosomal membrane damage and stress (Bonet-Ponce, et al., 2020; Eguchi, 2018), raising the possibility that manganese, through oxidative or metabolic mechanisms, may perturb endolysosomal integrity. While our earlier work showed that mutant LRRK2 sequesters Rab8a and other ERC proteins to damaged lysosomes (Mamais et al., 2021); here we show that manganese stress phenocopies aspects of that mislocalization even in wild-type LRRK2 contexts. These data support a model in which manganese induces spatial redistribution of Rab10 toward both centrosomal and lysosomal compartments, providing a mechanistic link between environmental stressors and PD-relevant vesicular dysfunction. Whether manganese exposure augments centrosomal cohesion and cilliogenesis deficits through LRRK2 kinase merits further investigation.

Our findings indicate that manganese activates LRRK2 through a redox-sensitive pathway involving mitochondrial dysfunction and mild membrane depolarization. While prior studies have shown that oxidative stress can enhance LRRK2 kinase activity and Rab substrate phosphorylation (Di Maio, 2018; Mamais et al., 2014), our data extend this by linking manganese-induced bioenergetic impairment to ROS accumulation and downstream LRRK2 activation. Importantly, we found that co-treatment with N-acetylcysteine suppressed Rab10 phosphorylation, underscoring the role of ROS as a proximal driver of LRRK2 signaling under manganese stress. Intriguingly, recent work by Keeney et al (Keeney, 2024) has shown that LRRK2 activity is not only responsive to ROS but can also actively promote ROS production by phosphorylating the p47^{phox} subunit of NADPH oxidase 2 (NOX2), thereby enhancing NOX2-dependent oxidative stress in cell and animal models of PD (Keeney, 2024). This raises the possibility that environmental toxicants like manganese may trigger a feedforward loop in which LRRK2 activation promotes ROS production, which in turn further activates LRRK2. Such a cycle could amplify oxidative damage and vesicular dysfunction over time, particularly in vulnerable neuronal populations. Recent studies highlight a role for LRRK2 in modulating cell vulnerability to ROS-induced damage leading to ferroptosis (Z, z., 2024; Oun et al., 2022). Together, these findings support a model in which LRRK2 functions both as a sensor and effector of redox imbalance, integrating environmental and metabolic cues to modulate PD-relevant cellular phenotypes.

We show that manganese exposure induces oxidative stress and activates LRRK2 kinase activity, which has been implicated in dopaminergic neurodegeneration. Notably, prior studies have shown that G2019S LRRK2 exacerbates manganese-induced neurotoxicity in dopaminergic neurons *in vivo* and LRRK2 inhibition rescues inflammasome activation microglia under these conditions (Pajarillo et al., 2023). Separately, LRRK2 inhibition was shown to attenuate manganese-induced expression of inflammatory cytokines and recover autophagic function of microglia (Chen et al., 2018). These data underscore the potential of LRRK2 inhibition as a therapeutic approach in environmentally linked parkinsonism and the importance in evaluating its neuroprotective efficacy in preclinical models of metal-induced PD.

Our findings show that metabolic and environmental stressors differentially regulate LRRK2 activity, leading to distinct patterns of Rab GTPase phosphorylation. These stressor-specific responses suggest that LRRK2 acts as a sensor of redox and metabolic signals, linking cellular stress to vesicular trafficking pathways. This highlights the importance of studying LRRK2 regulation in physiologically relevant contexts to better understand its role in PD pathogenesis.

4. Materials and Methods

4.1. Cell culture, treatments and constructs

HEK293T (R70007; Invitrogen) cells were maintained at 37 $^{\circ}$ C/ 5 $^{\circ}$

CO2 in high glucose Dulbecco's Modified Eagles Medium (DMEM) supplemented with 10 % (v/v) FBS (Gibco) and 2 mM L-glutamine (Thermo Fisher Scientific). Passage number was maintained below 20 to limit cellular stress. Inducible HEK293T cell lines expressing GFP LRRK2 were grown and cultured as described previously (Nichols et al., 2010). Cells were transfected with FLAG LRRK2 constructs using Lipofectamine 2000 using established protocols. The 3 × FLAG-tagged construct of LRRK2 in pCHMWS plasmid was a gift from Dr. J. M. Taymans (KU Leuven, Belgium) (Civiero, 2012). For metabolic stress treatments, cells were incubated in glucose-free media supplemented with 25 mM Glucose or 25 mM 2-Deoxy-Glucose for 4 h prior to one-hour treatment with DMSO, 1 μM Oligomycin A or 5 μM CCCP. In the calyculin A experiments, cells were treated with 10 nM calyculin A throughout the metabolic stress treatments as described above. In the manganese exposure experiments cells were treated with 100 µM MnCl₂ (Sigma; 63535) in complete media for 16 hrs. Mli-2 (Tocris; Cat. No. 5756) was used at 100 nM for 2 hrs. AICAR was used at 1 mM for 3 hr. Luminescent ATP content assay was done with the CellTiter-Glo kit (Promega). MLi-2 was purchased from Tocris Bioscience and dissolved in DMSO prior to use.

4.2. Primary astrocyte cultures

All procedures with animals followed the guidelines approved by the Institutional Animal Care and Use Committee of the National Institute on Aging. Astrocyte cultures were prepared from newborn (postnatal day 0-2) LRRK2 knockout (Lin, 2009), homozygous G2019S (Yue, 2015), homozygous R1441C (Tong, 2009) and wild-type mice. Dissected mouse cortices were incubated in 1 mL/cortex Basal Medium Eagle (BME) (Sigma-Aldrich), containing 5 U of papain/(Worthington) for 30 min at 37 $^{\circ}$ C. Five micrograms of deoxyribonuclease I was added to each cortex preparation, and brain tissue was dissociated into a cellular suspension that was washed twice with 10 volumes of BME and counted. Astrocyte cultures were plated in Dulbecco's modified Eagle's medium (DMEM) (Thermo Fisher Scientific), supplemented with 10 % fetal bovine serum (FBS) (Lonza) into 75-cm2 tissue culture flasks pre-coated with 50 µg/mL Poly-D-Lysine (Thermofisher). For the preparation of purified astrocyte cultures, 7- to 10-day primary cultures were vigorously shaken to detach microglia and oligodendrocytes. Cultures had >90 % of astrocytes in all experiments. Astrocytes were used from passage 2 to passage 3.

4.3. Quantification of LRRK2 dimerization and activity

To compare the effects of each metabolic stress on LRRK2 dimerization, we transfected HEK293T cells with LRRK2 fusion constructs as previously described (Leandrou et al., 2019). LRRK2 fused to biotin ligase (BirA-flag) or an acceptor peptide (AP) were expressed in cells under biotin-free conditions for 24 hr prior to induction of metabolic stress. At the termination of the stress period, the cells were washed 2X with PBS, followed by a brief biotin pulse (50 μM; 5 min, 37C). Following the biotin pulse, the cells were again extensively washed and pelleted in a $1.5\ mL$ centrifuge tube, and stored at $-80\C$ until use. Cell extracts were prepared, and 0.5 µg of protein was added to 96 well plates coated with streptavidin, to capture biotinylated LRRK2 dimers. Parallel plates were pre-coated with anti-LRRK2 (clone c41-2) antibodies to capture total expressed LRRK2 for normalization. The LRRK2 levels (dimeric or total) were determined by ELISA, using anti-LRRK2 (clone UDD3 or flag antibodies) and the dimeric LRRK2 expressed as a proportion of total expressed LRRK2. To measure the intrinsic kinase activity of purified LRRK2 dimers, we adapted the in-well kinase assay we previously described (Melachroinou et al., 2020) to the dimer-capture assay (Leandrou, 2019). Following capture of biotinylated LRRK2 dimers in SA-coated ELISA plates, kinase activity was measured by quantifying the phosphorylation of the NICtide peptide substrates by purified dimeric LRRK2. The signal arising from the phosphorylated

NICtide was normalized to the levels of dimeric LRRK2 determined by ${\it ELISA}$.

4.4. Immunocytochemistry

Cells were fixed in 4 % (w/v) formaldehyde/PBS for 15 min, permeabilized in 0.2 % Triton X-100/PBS for 10 min at RT, blocked in 5 % (v/v) FBS in PBS, and incubated with primary antibodies in 1 % (v/v) FBS/PBS overnight. Following 3 washes in PBS, the cells were incubated for 1 hr with secondary antibodies (Alexa Fluor 488, 568, 647-conjugated; ThermoFisher). After 3 PBS washes, the coverslips were mounted, and the cells were analyzed by confocal microscopy (Zeiss LSM 880 with Airyscan super-resolution, Nikon CSU-W1-SORA). The antibodies used were: pT73 RAB10 (MJF-R21-22–5; ab241060, Abcam), rat anti-FLAG (637301; BioLegend), Rab8a (Cell Signaling Technology; #6975), Lamp1 (DSHB; 1D4B), and Lamp2 (DSHB; H4B4). pT73 Rab10 levels were analyzed in FiJi (Schindelin et al., 2012) using the signal intensity of acquired image channels within the ROI of the cell perimeter.

4.5. Imaris analysis

Following confocal microscopy, the Imaris platform (Oxford Instruments) was used to visualize the localization of endogenous Rab8a in cells under metabolic stress. Z-stack confocal images were processed through the Imaris Surface Contour module to 3D render Rab8a tubular recycling endosomes.

4.6. Immunoblotting

Cells were lysed in ice-cold 1x Cell Signaling Lysis Buffer (Cell Signaling #9803S) supplemented with Halt phosphatase inhibitor cocktail (Thermofisher Scientific), and protease inhibitor cocktail (Roche) and left on ice for 30 min to lyse. Lysates were clarified at 20,000 g for 10 min at 4 degrees Celsius and pelleted debris were removed. Samples were supplemented with NuPage LDS sample buffer 4x (#NP0008), boiled for 5 min at 95 degrees Celsius and analyzed by standard western blot protocols using the following antibodies: GAPDH (Thermo Scientific, MA5-15738), FLAG (WB, Clone M2; F3165; Millipore-Sigma), Rabbit polyclonal against LRRK2 (MJFF2 c41-2; ab133474, Abcam), pS935-LRRK2 (ab133450; Abcam), pS1292-LRRK2 (MJFR-19-7-8, ab20318, abcam), pT73 Rab10 ([MJF-R21], ab230261, Abcam), pS106 Rab12 ([MJF-R25-9], ab256487, Abcam), RAB10 [ab237703 and ab104859, Abcam) Rab12 (18843-1-AP, ProteinTech), Cyclophilin B (ab16045, Abcam), AMPK (5831, Cell Signaling), pT172 AMPK (2535, Cell Signaling). Secondary antibodies were used at 1:10,000 dilution: IRDyes 800CW Goat anti-Rabbit IgG (LiCor; #926-32211) and 680RD Goat anti-Mouse IgG (LiCor; #926-68070).

4.7. XFe96 Seahorse Mito stress test

On the day before the assay, WT HEK293T cells (15,000 cells per well) were plated on Geltrex-coated Seahorse XFe96 culture plates. Cells were plated in media containing: DMEM containing no glucose, 10 % dialyzed FBS, 1 mM pyruvate, 1X glutamax, 50 $\mu g/$ mL uridine. Cells were either plated in media plus 25 mM glucose or no glucose (no carbon source) to ensure cellular dependence on mitochondrial OXPHOS for energy. Cells were treated overnight $\pm 100~\mu M$ MnCl $_2$. On the day of the experiment, the cartridge sensors were hydrated with XF calibrant and incubated for 4 hr at 37 °C in a non-CO $_2$ incubator. The cells were washed (~14 h post-plating) to remove traces of FBS in DMEM XF assay medium containing 1 mM pyruvate and 2 mM glutamine. Post-wash, the cells were resuspended in a final volume of 180 μl DMEM XF assay medium containing 1 mM pyruvate, 2 mM glutamine, and glucose (25 mM or none) and MnCl $_2$ (100 μl or none), consistent with the treatment

conditions. The cell culture plate was incubated for 2.5 hr at 37 °C in a non-CO2 incubator prior to loading into a XFe96 analyzer. A standard mito stress test program was run with the following final concentrations of inhibitors per well: glucose-containing medium (1 μ M oligomycin, 1 μM FCCP, 0.5 μM Rotenone + Antimycin A) and no glucose medium (1 μM oligomycin, 2.5 μM FCCP, 0.5 μM Rotenone + Antimycin A). Four measurements were taken before and after each inhibitor injection. Postassay completion, readings were normalized to cell count by staining for nuclei with 1 µg/ mL Hoescht and imaging in the high content microscope Lionheart FX (Agilent). The traces for oxygen consumption rate (OCR) normalized to cell count are represented as mean \pm SEM of n =12 wells. The following parameters were calculated as follows: Basal respiration = Last measurement #4 before first oligomycin injection minimum rate measurement #16 after rotenone / antimycin A injection; Maximal respiration = maximum rate measurement #9 after FCCP injection – minimum rate measurement #16 after rotenone / antimycin A injection; Proton leak = first measurement #5 after oligomycin injection - minimum rate measurement #16; ATP-dependent OCR = Last measurement #4 before first oligomycin injection - first measurement #5 after oligomycin injection; Coupling efficiency = ATP-dependent OCR / Basal respiration *100; Spare respiratory capacity = maximum rate measurement #9 after FCCP injection - Last measurement #4 before first injection. The data is represented as mean \pm SEM of n = 12. The Statistical analysis was conducted by one-way ANOVA with Tukey's post-hoc analysis: * p < 0.05, ** p < 0.01, *** p < 0.001.

4.8. Animals

All animal protocols were approved by the Gerontology Research Center Animal Care and Use Committee (339-DKI-Ra) of the National Institute on Aging, NIH. The NIA IRP maintains an assurance with the Office of Laboratory Animal Welfare (OLAW) via the Office of Animal Care and Use (OACU) of the NIH. The NIA IRP complies with standards of the Guide for the Care and Use of Laboratory Animals, NRC, 2011, and the PHS Policy on Humane Care and Use of Laboratory Animals, USDHHS, NIH, OLAW, 2015 for all animals, as well as the Animal Welfare Act, USDA, regulations and USDA Animal Care Policies for USDA's Animal Welfare Act, USDA, APHIS. The 2DG in vivo cohort has been characterized before (Minor et al., 2010). 3-month old male rats were housed individually in clear plastic cages on a 12:12 h light:dark schedule at the Holabird NIA/NIH research facility in Baltimore, MD, with food and water available ad libitum. After a 6-day habituation period, the rats were weighed and randomly assigned to dietary treatment groups to receive NIH-31 standard rodent chow (Harlan Teklad, Indianapolis, IN, USA) supplemented by dry weight with 0.6 %, 0.2 % or 0.04 % Sigma 2DG, or unsupplemented NIH-31 chow. Throughout the duration of the study, all rats had ad libitum access to weighed amounts of their prescribed diet and water. At the end of the 6-week feeding period, the rats were euthanized and brain and kidney were flash frozen for further analysis.

4.9. Statistics

Experiments examining phosphorylation levels of LRRK2 and Rab GTPases by immunoblotting and Rab10 phosphorylation by ICC were analyzed by one-way ANOVA with Tukey's post hoc test or two-tailed Student's t-test as indicated in the figure legends. All statistical analyses were performed using GraphPad Prism for Windows (GraphPad Software, San Diego, CA). Mean values \pm S.E. are indicated.

CRediT authorship contribution statement

Michalis Kentros: Methodology, Investigation, Formal analysis, Data curation. **Jordan Follett:** Formal analysis, Methodology, Writing – review & editing. **Nitya Subrahmanian:** Writing – original draft, Methodology, Investigation, Formal analysis. **Aravindraja**

Chairmandurai: Methodology, Formal analysis, Data curation. Katerina Melachroinou: Formal analysis, Data curation. Diane B. Re: Investigation, Formal analysis, Data curation. Rafael de Cabo: Writing review & editing. Ruth Chia: Writing - review & editing, Investigation, Formal analysis. Jillian H. Kluss: Writing - review & editing, Investigation, Funding acquisition, Formal analysis. Alexandra Beilina: Formal analysis, Data curation. **Heather Mortiboys:** Writing – review & editing, Formal analysis. Matthew J. LaVoie: Writing - review & editing, Writing - original draft. Hardy J. Rideout: Writing - review & editing, Writing - original draft, Supervision, Project administration, Methodology, Formal analysis, Data curation, Conceptualization. Mark R. Cookson: Writing - review & editing, Writing - original draft, Investigation, Conceptualization. Adamantios Mamais: Writing - review & editing, Writing - original draft, Visualization, Supervision, Resources, Project administration, Methodology, Investigation, Funding acquisition, Formal analysis, Data curation, Conceptualization.

Declaration of competing interest

The authors declare that they have no known competing financial interests or personal relationships that could have appeared to influence the work reported in this paper.

Acknowledgements

This work was supported in part by the Michael J. Fox Foundation for Parkinson's Research (MJFF) grant MJFF-023425 (A.M., M.J.L.), National Institutes of Health grants NS110188 and AG082373 (M.J.L.) and AG077269 (A.M.) and the Intramural Research Program of the NIH, National Institute on Aging.

Appendix A. Supplementary data

Supplementary data to this article can be found online at https://doi.org/10.1016/j.brainres.2025.149785.

Data availability

Data will be made available on request.

References

Ang, A.L., et al., 2004. Recycling endosomes can serve as intermediates during transport from the Golgi to the plasma membrane of MDCK cells. J. Cell Biol. 167, 531–543.
Beilina, A., et al., 2014. Unbiased screen for interactors of leucine-rich repeat kinase 2 supports a common pathway for sporadic and familial Parkinson disease. Proc. Natl. Acad. Sci. U.S.A. 111, 2626–2631.

Berger, Z., Smith, K.A., Lavoie, M.J., 2010. Membrane localization of LRRK2 is associated with increased formation of the highly active LRRK2 dimer and changes in its phosphorylation. Biochemistry 49, 5511–5523.

Biosa, A., et al., 2013. GTPase activity regulates kinase activity and cellular phenotypes of Parkinson's disease-associated LRRK2. Hum. Mol. Genet. 22, 1140–1156.

Bonet-Ponce, L., et al. LRRK2 mediates tubulation and vesicle sorting from membrane damaged lysosomes. bioRxiv 2020.01.23.917252 (2020) doi:10.1101/ 2020.01.23.917252.

Booth, H.D.E., Hirst, W.D., Wade-Martins, R., 2017. The role of astrocyte dysfunction in Parkinson's disease pathogenesis. Trends Neurosci. 40, 358–370.

Brown, T.C., Correia, S.S., Petrok, C.N., Esteban, J.A., 2007. Functional compartmentalization of endosomal trafficking for the synaptic delivery of AMPA receptors during long-term potentiation. J. Neurosci. 27, 13311–13315.

Bu, M., et al., 2023. Inhibition of LRRK2 kinase activity rescues deficits in striatal dopamine physiology in VPS35 p.D620N knock-in mice. Npj Parkinsons. Dis. 9, 1–12.

Burtey, A., et al., 2015. Intercellular transfer of transferrin receptor by a contact-, Rab8-dependent mechanism involving tunneling nanotubes. FASEB J. 29, 4695–4712.

Casamayor, A., Ariño, J., 2020. Controlling Ser/Thr protein phosphatase PP1 activity and function through interaction with regulatory subunits. Adv. Protein Chem. Struct. Biol. 122, 231–288.

Chen, J., Su, P., Luo, W., Chen, J., 2018. Role of LRRK2 in manganese-induced neuroinflammation and microglial autophagy. Biochem. Biophys. Res. Commun. 498, 171–177.

Chia, R., et al., 2014. Phosphorylation of LRRK2 by casein kinase 1α regulates trans-Golgi clustering via differential interaction with ARHGEF7. Nat. Commun. 5, 5827.

- Chittoor-Vinod, V.G., et al., 2020. Dietary amino acids impact LRRK2-induced neurodegeneration in Parkinson's disease models. J. Neurosci. 40, 6234–6249.
- Choi, S.-W., Song, J.-K., Yim, Y.-S., Yun, H.-G., Chun, K.-H., 2015. Glucose deprivation triggers protein kinase C-dependent β-catenin proteasomal degradation. J. Biol. Chem. 290, 9863–9873.
- Civiero, L., et al., 2012. Biochemical characterization of highly purified leucine-rich repeat kinases 1 and 2 demonstrates formation of homodimers. PLoS One 7, e43472.
- Cook, D.A., et al., 2017. LRRK2 levels in immune cells are increased in Parkinson's disease. Npj Parkinson's Disease 3, 1–12.
- Covy, J.P., Giasson, B.I., 2010. The G2019S pathogenic mutation disrupts sensitivity of leucine-rich repeat kinase 2 to manganese kinase inhibition. J. Neurochem. 115, 36-46
- Deo, R., et al., 2018. ATP-dependent membrane remodeling links EHD1 functions to endocytic recycling. Nat. Commun. 9, 5187.
- Dhekne, H.S., et al., 2018. A pathway for Parkinson's Disease LRRK2 kinase to block primary cilia and Sonic hedgehog signaling in the brain. Elife 7, e40202.
- Di Maio, R., et al., 2018. LRRK2 activation in idiopathic Parkinson's disease. Sci. Transl. Med. 10.
- Diessl, J., et al., 2022. Manganese-driven CoQ deficiency. Nat Commun. 13, 6061.Dzamko, N., et al., 2012. The IkappaB kinase family phosphorylates the Parkinson's disease kinase LRRK2 at Ser935 and Ser910 during Toll-like receptor signaling. PLoS One 7, e39132.
- Eguchi, T., et al., 2018. LRRK2 and its substrate Rab GTPases are sequentially targeted onto stressed lysosomes and maintain their homeostasis. Proc. Natl. Acad. Sci. U. S. A. 115, E9115–E9124.
- Esseltine, J.L., Ribeiro, F.M., Ferguson, S.S.G., 2012. Rab8 modulates metabotropic glutamate receptor subtype 1 intracellular trafficking and signaling in a protein kinase C-dependent manner. J. Neurosci. 32, 16933–16942.
- Fernandes, J., et al., 2017. From the cover: manganese stimulates mitochondrial H2O2 production in SH-SY5Y human neuroblastoma cells over physiologic as well as toxicologic range. Toxicol. Sci. 155, 213–223.
- Garcia-Haro, L., et al., 2010. The PP1-R6 protein phosphatase holoenzyme is involved in the glucose-induced dephosphorylation and inactivation of AMP-activated protein kinase, a key regulator of insulin secretion, in MIN6 beta cells. FASEB J. 24, 5080-5091.
- Greggio, E., et al., 2006. Kinase activity is required for the toxic effects of mutant LRRK2/ dardarin. Neurobiol. Dis. 23, 329–341.
- Gustavsson, E.K., et al., 2024. RAB32 Ser71Arg in autosomal dominant Parkinson's disease: linkage, association, and functional analyses. Lancet Neurol. 23, 603–614.
- Hardie, D.G., 2011. AMP-activated protein kinase—an energy sensor that regulates all aspects of cell function. Genes Dev. 25, 1895–1908.
- Harischandra, D.S., et al., 2019. Manganese-induced neurotoxicity: new insights into the triad of protein misfolding, mitochondrial impairment, and neuroinflammation. Front. Neurosci. 13.
- Hattula, K., et al., 2006. Characterization of the Rab8-specific membrane traffic route linked to protrusion formation. J. Cell Sci. 119, 4866–4877.
- Homma, Y., Fukuda, M., 2016. Rabin8 regulates neurite outgrowth in both GEF activity-dependent and -independent manners. Mol. Biol. Cell 27, 2107–2118.
- Hsieh, C.-H., et al., 2016. Functional impairment in miro degradation and mitophagy is a shared feature in familial and sporadic Parkinson's disease. Cell Stem Cell 19, 709–724.
- Ingram, D.K., et al., 2006. Calorie restriction mimetics: an emerging research field. Aging Cell $5,\,97-108$.
- Kania, E., et al., 2023. LRRK2 phosphorylation status and kinase activity regulate (macro)autophagy in a Rab8a/Rab10-dependent manner. Cell Death Dis. 14, 1–14.
- Ke, R., Xu, Q., Li, C., Luo, L., Huang, D., 2018. Mechanisms of AMPK in the maintenance of ATP balance during energy metabolism. Cell Biol. Int. 42, 384–392.
- Keeney, M.T., et al., 2024. LRRK2 regulates production of reactive oxygen species in cell and animal models of Parkinson's disease. Sci. Transl. Med. 16, eadl3438.
- Kim, J., et al., 2019. LRRK2 kinase plays a critical role in manganese-induced inflammation and apoptosis in microglia. PLoS One 14, e0210248.
- Kim, J., et al., 2023. LRRK2 attenuates antioxidant response in familial Parkinson's disease derived neural stem cells. Cells 12, 2550.
- Kim, J., Kundu, M., Viollet, B., Guan, K.-L., 2011. AMPK and mTOR regulate autophagy through direct phosphorylation of Ulk1. Nat. Cell Biol. 13, 132–141.
- Kluss, J.H., Mamais, A., Cookson, M.R., 2019. LRRK2 links genetic and sporadic Parkinson's disease. Biochem. Soc. Trans. 47, 651–661.
- Kobayashi, H., Etoh, K., Ohbayashi, N., Fukuda, M., 2014. Rab35 promotes the recruitment of Rab8, Rab13 and Rab36 to recycling endosomes through MICAL-L1 during neurite outgrowth. Biology Open 3, 803–814.
- Kwakye, G.F., Paoliello, M.M.B., Mukhopadhyay, S., Bowman, A.B., Aschner, M., 2015. Manganese-induced parkinsonism and Parkinson's disease: shared and distinguishable features. Int. J. Environ. Res. Public Health 12, 7519–7540.
- Lara Ordónez, A.J., et al., 2019. RAB8, RAB10 and RILPL1 contribute to both LRRK2 kinase-mediated centrosomal cohesion and ciliogenesis deficits. Hum. Mol. Genet. 28, 3552-3568.
- Leandrou, E., et al., 2019. Kinase activity of mutant LRRK2 manifests differently in hetero-dimeric vs. homo-dimeric complexes. Biochem. J 476, 559–579.
- Lewis, P.A., et al., 2007. The R1441C mutation of LRRK2 disrupts GTP hydrolysis. Biochem. Biophys. Res. Commun. 357, 668–671.
- Li, H., et al., 2017. Rab8A regulates insulin-stimulated GLUT4 translocation in C2C12 myoblasts. FEBS Lett. 591, 491–499.
- Lin, X., et al., 2009. Leucine-rich repeat kinase 2 regulates the progression of neuropathology induced by Parkinson's disease-related mutant α -synuclein. Neuron 64, 807.

Lobbestael, E., et al., 2013. Identification of protein phosphatase 1 as a regulator of the LRRK2 phosphorylation cycle. Biochem. J 456, 119–128.

- Lovitt, B., et al., 2010. Differential effects of divalent manganese and magnesium on the kinase activity of leucine-rich repeat kinase 2 (LRRK2). Biochemistry 49, 3092–3100.
- Madero-Pérez, J., et al., 2018. Parkinson disease-associated mutations in LRRK2 cause centrosomal defects via Rab8a phosphorylation. Mol. Neurodegener. 13, 3.
- Mamais, A., et al., 2014. Arsenite stress down-regulates phosphorylation and 14-3-3 binding of leucine-rich repeat kinase 2 (LRRK2), promoting self-association and cellular redistribution. J. Biol. Chem. 289, 21386–21400.
- Mamais, A., et al., 2021. Mutations in LRRK2 linked to Parkinson disease sequester Rab8a to damaged lysosomes and regulate transferrin-mediated iron uptake in microglia. PLoS Biol. 19, e3001480.
- Mamais, A., et al., 2024. The LRRK2 kinase substrates RAB8a and RAB10 contribute complementary but distinct disease-relevant phenotypes in human neurons. Stem Cell Rep. 19, 163–173.
- Martinez Fiesco, J.A. et al. 14-3-3 binding maintains the Parkinson's associated kinase LRRK2 in an inactive state. bioRxiv 2024.11.22.624879 (2024) doi:10.1101/2024.11.22.624879.
- Melachroinou, K., et al., 2020. Elevated in vitro kinase activity in peripheral blood mononuclear cells of leucine-rich repeat kinase 2 G2019S carriers: a novel enzymelinked immunosorbent assay-based method. Mov. Disord. 35, 2095–2100.
- Minor, R.K., et al., 2010. Chronic ingestion of 2-deoxy-D-glucose induces cardiac vacuolization and increases mortality in rats. Toxicol. Appl. Pharmacol. 243, 332–339.
- Mir, R., et al., 2018. The Parkinson's disease VPS35[D620N] mutation enhances LRRK2-mediated Rab protein phosphorylation in mouse and human. Biochem. J 475, 1861–1883.
- Moore, F., Weekes, J., Hardie, D.G., 1991. Evidence that AMP triggers phosphorylation as well as direct allosteric activation of rat liver AMP-activated protein kinase. Eur. J. Biochem. 199, 691–697.
- Morcillo, P., et al., 2021. Defective mitochondrial dynamics underlie manganese-induced neurotoxicity. Mol. Neurobiol. 58, 3270–3289.
- Mortiboys, H., et al., 2015. UDCA exerts beneficial effect on mitochondrial dysfunction in LRRK2(G2019S) carriers and in vivo. Neurology 85, 846–852.
- Most, J., Tosti, V., Redman, L.M., Fontana, L., 2016. Calorie restriction in humans: an update. Ageing Res. Rev. https://doi.org/10.1016/j.arr.2016.08.005.
- Nichols, R.J., et al., 2010. 14-3-3 binding to LRRK2 is disrupted by multiple Parkinson's disease-associated mutations and regulates cytoplasmic localization. Biochem. J 430, 393–404.
- Oun, A., et al., 2022. LRRK2 protects immune cells against erastin-induced ferroptosis. Neurobiol. Dis. 175, 105917.
- Pagliarani, A., Nesci, S., Ventrella, V., 2013. Modifiers of the oligomycin sensitivity of the mitochondrial F1F0-ATPase. Mitochondrion 13, 312–319.
- Pajarillo, E., et al., 2023. The role of microglial LRRK2 kinase in manganese-induced inflammatory neurotoxicity via NLRP3 inflammasome and RAB10-mediated autophagy dysfunction. J. Biol. Chem. 299.
- Papkovskaia, T.D., et al., 2012. G2019S leucine-rich repeat kinase 2 causes uncoupling protein-mediated mitochondrial depolarization. Hum. Mol. Genet. 21, 4201–4213.
- Park, J.-M., Lee, D.-H., Kim, D.-H., 2023. Redefining the role of AMPK in autophagy and the energy stress response. Nat. Commun. 14, 2994.
- Peres, T.V., et al., 2016. Manganese-induced neurotoxicity: a review of its behavioral consequences and neuroprotective strategies. BMC Pharmacol. Toxicol. 17, 57.
- Pfeffer, S.R., 2023. LRRK2 phosphorylation of Rab GTPases in Parkinson's disease. FEBS Lett. 597, 811–818.
- Quadri, M., et al., 2012. Mutations in SLC30A10 cause parkinsonism and dystonia with hypermanganesemia, polycythemia, and chronic liver disease. Am. J. Hum. Genet. 90, 467–477
- Raig, N. D. *et al.* Type-II kinase inhibitors that target Parkinson's Disease-associated LRRK2. 2024.09.17.613365 Preprint at https://doi.org/10.1101/2024.09.17.613365 (2025).
- Rao, K.V.R., Norenberg, M.D., 2004. Manganese induces the mitochondrial permeability transition in cultured astrocytes*. J. Biol. Chem. 279, 32333–32338.
- Riou, P., et al., 2013. 14-3-3 proteins interact with a hybrid prenyl-phosphorylation motif to inhibit G proteins. Cell 153, 640–653.
- Schapansky, J., Nardozzi, J.D., Felizia, F., LaVoie, M.J., 2014. Membrane recruitment of endogenous LRRK2 precedes its potent regulation of autophagy. Hum. Mol. Genet. 23, 4201–4214.
- Schindelin, J., et al., 2012. Fiji: an open-source platform for biological-image analysis. Nat. Methods 9, 676–682.
- Schiweck, J., et al., 2021. Drebrin controls scar formation and astrocyte reactivity upon traumatic brain injury by regulating membrane trafficking. Nat. Commun. 12, 1490.
- Schmidt, S.H., et al., 2019. The dynamic switch mechanism that leads to activation of LRRK2 is embedded in the DFG ψ motif in the kinase domain. Proc. Natl. Acad. Sci. U. S. A. 116, 14979–14988.
- Sharma, M., Giridharan, S.S.P., Rahajeng, J., Naslavsky, N., Caplan, S., 2009. MICAL-L1 links EHD1 to tubular recycling endosomes and regulates receptor recycling. Mol. Biol. Cell 20, 5181–5194.
- Smith, M.R., Fernandes, J., Go, Y.-M., Jones, D.P., 2017. Redox dynamics of manganese as a mitochondrial life-death switch. Biochem. Biophys. Res. Commun. 482, 388–398.
- Steger, M., et al. Phosphoproteomics reveals that Parkinson's disease kinase LRRK2 regulates a subset of Rab GTPases. eLife 5, (2016).
- Stein, S.C., Woods, A., Jones, N.A., Davison, M.D., Carling, D., 2000. The regulation of AMP-activated protein kinase by phosphorylation. Biochem. J 345, 437–443.

M. Kentros et al.

- Sun, Y., Connors, K.E., Yang, D.-Q., 2007. AICAR induces phosphorylation of AMPK in an ATM-dependent, LKB1-independent manner. Mol. Cell. Biochem. 306, 239–245.
- Tasegian, A., Singh, F., Ganley, I.G., Reith, A.D., Alessi, D.R., 2021. Impact of type II LRRK2 inhibitors on signalling and mitophagy. Biochem. J. https://doi.org/ 10.1042/BCJ20210375.
- Tong, Y., et al., 2009. R1441C mutation in LRRK2 impairs dopaminergic neurotransmission in mice. Proc. Natl. Acad. Sci. U. S. A. 106, 14622–14627.
- Trilling, C.R., et al., 2024. RedOx regulation of LRRK2 kinase activity by active site cysteines. Npj Parkinsons. Dis. 10, 1–11.
- Wall, A.A., et al., 2017. Small GTPase Rab8a-recruited phosphatidylinositol 3-kinase γ regulates signaling and cytokine outputs from endosomal toll-like receptors. J. Biol. Chem. 292, 4411–4422.
- Wunderley, L., et al., 2021. Endosomal recycling tubule scission and integrin recycling involve the membrane curvature-supporting protein LITAF. J. Cell Sci. 134, jcs258549.
- Yang, D., et al., 2012. LRRK2 kinase activity mediates toxic interactions between genetic mutation and oxidative stress in a Drosophila model: suppression by curcumin. Neurobiol. Dis. 47, 385–392.
- Yao, L., et al., 2023. LRRK2 Gly2019Ser mutation promotes ER stress via interacting with THBS1/TGF- β 1 in Parkinson's disease. Adv. Sci. (weinh) 10, e2303711.
- Yao, L., et al., 2025. Translational evaluation of metabolic risk factors impacting DBS efficacy for PD-related sleep and depressive disorders: preclinical, prospective and cohort studies. Int. J. Surg. 111, 543–566.
- Yoshimura, S.-I., Egerer, J., Fuchs, E., Haas, A.K., Barr, F.A., 2007. Functional dissection of Rab GTPases involved in primary cilium formation. J. Cell Biol. 178, 363–369.
- Yue, M., et al., 2015. Progressive dopaminergic alterations and mitochondrial abnormalities in LRRK2 G2019S knock-in mice. Neurobiol. Dis. 78, 172–195.
- Z, Z., et al., 2024. LRRK2 regulates ferroptosis through the system Xc-GSH-GPX4 pathway in the neuroinflammatory mechanism of Parkinson's disease. J. Cell. Physiol. 239.